Annu. Rev. Fluid Mech. 1992. 24 : 313–58

HYDRODYNAMIC PHENOMENA IN SUSPENSIONS OF SWIMMING MICROORGANISMS

T. J. Pedley

Department of Applied Mathematical Studies, University of Leeds, Leeds LS2 9JT, England

J. O. Kessler

Department of Physics, University of Arizona, Tucson, Arizona 85721

KEY WORDS: bioconvection, pattern formation, algae, bacteria, gyrotaxis

1. INTRODUCTION

Vast numbers of microorganisms are suspended in temperate aqueous environments. Oceans and rivers, puddles and droplets, the fluid interiors of animals, all host an array of splendidly varied creatures. Although their presence is usually not casually obvious, they constitute the major part of the world's biomass. Their population dynamics—replication and decay, accumulation and dispersal—modulates and regulates their own life, the life of the larger creatures that feed on them, and even the climate (Charlson et al 1987). Microorganisms interact with each other and with the world, at length scales that vary upward from the size of an individual, say 10^{-4} cm, to the dimensions of the entire body of fluid in which they live.

Fluid mechanics, in concert with the organisms' behavior, governs the dynamics of many of these interactions. However, we are concerned here with relatively localized, small-scale phenomena. We consider only single-celled microorganisms which are motile, i.e. self-propelled, and so small that inertial effects can be ignored in describing their locomotion. Examples to be discussed include species of algae, bacteria, and protozoa, not to mention spermatozoa.

The trajectories along which individual cells swim are determined by the

0066-4189/92/0115–0313$02.00

swimming velocity vector, relative to the fluid, coupled with advection by the fluid flow. The swimming velocity is itself oriented by fluid mechanical and environmental influences of various kinds. Concentrated populations of cells can modify the environmental influences acting on a given cell, e.g. by shading from the light or by consuming nutrients; they can also modify the ambient fluid velocity field, through convection currents driven by nonuniformities in the cell concentration.

A concentrated population of suspended cells is a nonlinear dynamical system. As such, it is a generator of spatial and temporal patterns that are both physically fascinating and potentially of great biological significance. This article summarizes the progress made thus far in understanding the system, tracing the thread from individual to collective dynamics.

2. PROPERTIES OF SWIMMING MICROORGANISMS

2.1 *Shape and Behavior*

We consider microorganisms that swim and are small enough for inertial effects to be ignored in an individual's locomotion. This group includes bacteria, spermatozoa and other gametes, unicellular and colonial algae, and protozoans. Names of some typical genera (excluding gametes) are, respectively, *Bacillus*, *Chlamydomonas*, *Volvox*, and *Tetrahymena.* Their mean diameters lie in the range from 1 to 200 μm. The organisms considered are denser than the water in which they swim, by a few percent for the algae, approximately 10% for bacteria such as *B. subtilis* (Hart & Edwards 1987), and 30% for spermatozoa (Bretherton & Rothschild 1961).

Microorganisms propel themselves through the water by using waving, undulating, or rotating appendages, called flagella or cilia, which are arranged in various geometries. Swimming speeds (V_s) range up to several hundred μm s^{-1}. The Reynolds number based on V_s and diameter d of individuals is usually less than 10^{-2}. There is a very great diversity of microorganism shapes (e.g. Bold & Wynne 1978, Pelczar et al 1986, Prescott et al 1990). The fluid habitats of swimmers range from soil moisture and melting snow to lakes, oceans, and even saturated saline ponds. The bloodstream, digestive, and reproductive canals of animals are enclosed fluid environments which also house motile microorganisms. Within any particular environment the successful motile forms often vary greatly.

In this article we concentrate attention on a few cell types, one in particular: a spheroid that swims by a breaststroke-like motion of two flagella, which are attached near the anterior end (Rüffer & Nultsch 1985). The mass distribution is typically anisotropic, so that the center of mass

is posterior to the center of buoyancy. There are many genera of algae having this general form. Many others which do not, such as the Euglenas (Leedale 1967) and Dinoflagellates, nevertheless exhibit similar physical behavior patterns to those of the genus *Chlamydomonas* ($d = 10$–20 μm, $V_s = 50$–100 μm s^{-1}) from which the generic body pattern adopted here is derived. We believe, therefore, that the simplification achieved by analyzing mainly one generic type of algal cell is appropriate.

We shall in addition consider the larger ciliated protozoan, *Tetrahymena pyriformis*, often used in bioconvection studies (Section 4). This has a typical diameter d of 35 μm and swimming speed $V_s \approx 500$ μm s^{-1}. At the other end of the size range we shall take the "typical" bacterium to be *Bacillus subtilis*, rather elongated (length $\simeq 2$
propelled by a rotating flagellum at the rear (V_s up to ~ 20 μm s^{-1}). One further general shape, a small body (head) propelled by a long tail, appears in many cells. They include spermatozoa and swarmer cells involved in reproduction of (for example) fungi, macro-algae, echinoderms, and mammals. Spermatozoa typically have a dense head with a volume of 6 μm^3 and a tail up to 50 μm long (Bretherton & Rothschild 1961); they swim with speed V_s in the range 80–250 μm s^{-1} (Bishop 1962). Some bacteria are also propelled by a single polar flagellum. One spectacular case is *Bdellovibrio bacteriovorans*. It swims at the rate of 100 cell body lengths per second. The cell body is 1.5 μm long $\times$ 0.3 μm diameter, the tail length is ~ 4 μm. This predator cell bores into larger bacteria by rotating its "head" at 6000 rpm (Neidhardt et al 1990). Other examples of a body propelled by a postcrior flagellum are the small alga *Pedinomonas* (Bold & Wynne 1978), and the Trypanosomes (Pelczar et al 1986), which are protozoa that live in the bloodstream of mammals, causing sleeping sickness and Chagas' disease.

One of the most interesting aspects of microorganism locomotion is cell rotation, approximately around the direction of locomotion. As seen from the rear, most species of bacteria rotate clockwise about the swimming direction **p**, in order to balance the torque of their counterclockwise rotating flagella (Berg 1983, Prescott et al 1990). Algal cells exhibit many distinct swimming styles, but cells of a given species all rotate in the same direction as a result of a genetically determined asymmetry of their flagellar attachments (Melkonian 1989, Floyd & O'Kelley 1989). All of the many species of dinoflagellates rotate clockwise (Levandowsky & Kaneta 1987).

ORIENTATION MECHANISMS Microorganisms respond to stimuli by swimming, on average, in particular directions. Such responses are called *taxes*. Taxes of importance in this article are *gravitaxis* (or *geotaxis*), a response to gravity or acceleration; *phototaxis*, a response to light; and *chemotaxis*,

a response to chemical gradients. Responses to shear in the ambient flow are sometimes called *rheotaxis* (see footnote to Section 3.1). Compensating torques due to shear and gravity produce *gyrotaxis*. Some bacteria contain magnetic particles (magnetosomes), which cause them to swim along magnetic field lines (*magnetotaxis*).

Gravitaxis causes many organisms to swim vertically upwards, on average, in still water; this is particularly true for photosynthetic algae. Some of the more complex protozoa have a primitive gravity-sensing device. *Loxodes* (Fenchel & Finlay 1984, 1986) has an internal weighted lever, whose position, together with the local oxygen concentration, appears to control the swimming direction. As previously mentioned, the simplest mechanism for responding to the gravitational field is to have an asymmetric mass distribution, so the center of mass G is displaced from the center of buoyancy B. The consequent gravitational torque tends to keep G below B. If the cell swims in the direction $\overrightarrow{GB}$ it will swim upwards. Various species of algae are bottom-heavy and swim upwards in this way.

The easily visible off-axis chloroplast of the nearly spherical biflagellated alga *Chlamydomonas oligochloris* (Ettl 1976) causes the center of mass also to be located well off the symmetry axis of the cell. The cell rotates approximately around its symmetry axis while it swims. This rotation, acting in concert with the gravitational torque, causes the cell to swim upward on average, yet with a pronounced wobble superimposed on its mean progress. The resultant motion is quite common; it probably indicates a dynamically equivalent morphology. The dinoflagellate *Peridinium* is another case where the wobble is marked, but the mass anisotropy has not been observed.

Most green, photosynthetic, motile algae, whether or not they are bottom-heavy, are phototactic to some extent (Haupt & Feinleib 1979, Nultsch & Häder 1988). Some always swim towards the brightest light; most, such as *Euglena* or *Chlamydomonas* swim towards a weak light but away from a strong one [leading them to form interesting patterns as they seek to shelter behind each other (Wager 1911, Kessler 1986a)]. Negative phototaxis—the tendency to swim away from strong light—is sufficient to overcome negative gravitaxis (Häder 1987). Physical and physiological orienting mechanisms occur simultaneously and ought to add in a manner that is useful to the organism. In many algal species phototaxis exploits the rotation that accompanies locomotion (Colombetti & Lenci 1983). The mechanism depends on the intermittent shading of a centrally-located photoreceptor by an opaque region, called a stigma or eyespot, which is located near the outer surface of the cell. When the cell rotates with its axis transverse to a beam of light, the eyespot intermittently interrupts the illumination. When the cell's rotation axis is parallel to the light, the

modulation ceases. This mechanism, together with intensity information, serves to guide the cell relative to the light beam. The eyespot usually consists of a patch of pigment, but on occasions it is a diffraction grating (Foster & Smyth 1980). There are various other rather complex responses to illumination (Häder & Tevini 1987). For example, the reaction of cells to spatial or temporal variations in light intensity often includes start/stop behavior ("photophobic responses"). A complete theory of strongly illuminated bioconvection patterns will have to include such effects.

A variety of mechanisms can cause microorganism populations to accumulate in regions of space that have particular properties. These mechanisms include changes of swimming style or speed, modulation of intermittent activities such as random reorientations, or taxis, which is oriented locomotion. Thermotaxis of *Paramecium* is an example of such an accumulative effect (Tsuchiya & Kawakubo 1981). This discussion is included as a warning to the reader that "*C*-taxis" need not mean direct locomotion along $\pm$ grad C.

The accumulation (or depletion) of bacterial cells in gradients of chemical concentration is classified as chemotaxis. It seems obvious that an organism 1–2 μm long is unlikely to be able within itself to sense a chemical concentration (C) gradient with a length scale of millimeters. Various other models have been proposed. Since many bacteria are known to swim in straight line bursts, separated by random reorientations (Berg & Brown 1972) and pauses (Armitage & Macnab 1987, Lapidus et al 1988), they could arrange for the bursts to be longer when appropriately directed. Another possibility, that more vigorous but totally random swimming in a region of higher C could lead to a C-dependent effective cell diffusivity D and hence to a net cell flux, does not work because the flux is inevitably from the region of higher D to that of lower D (Schnitzer et al 1990). Of course, cells could accumulate by swimming more slowly in the "desired" region. Many bacteria swim up and down oxygen gradients, toward a preferred concentration. The kinetics of this *aerotaxis* is not as well understood as other bacterial chemotaxes, although the mechanism is sometimes quite similar (Shioi et al 1987). Depending on concentration, oxygen can be either a metabolic requirement or a poison. One would therefore expect that response to it would be different from response to other chemicals that have less physiological importance. Optimal oxygen concentrations—often in the middle of a concentration gradient—are reproducibly occupied by bacteria (Taylor 1983, Nelson et al 1986), as well as by large ciliated microorganisms (Finlay et al 1987). The consumption of oxygen by swimming organisms, coupled with their aerotactic response to concentration, excites spectacular spatial and temporal fluid dynamical patterns (see Section 4).

In a shear flow, with both vorticity and strain-rate, elongated cells have a preferred orientation aligned with the streamlines. The associated accumulative behavior is called rheotaxis, especially in the context of spermatozoon motility investigations (Rothschild 1962, Bretherton & Rothschild 1961, Roberts 1970). The joint effect of shear alignment and another orienting influence can lead to orientation and therefore swimming in a direction different from that which would result from either influence separately. For example, bottom-heavy cells in a flow with horizontal vorticity tend to swim at an angle to the vertical, a process known as gyrotaxis. The combination of viscous and other orienting torques is discussed fully in the next section.

The typical nose-heavy shape of spermatozoa suggests that these cells ought to be positively gravitactic (Roberts 1972, Katz & Pedrotti 1977, Winet et al 1984). That thought has spawned many attempts to separate X from the somewhat lighter Y chromosome-bearing spermatozoa. Winet et al review some of these efforts and show experimentally that gravitaxis is remarkably weak in human spermatozoa (see Section 3.1).

ENERGY The energy stored within microorganisms is acquired by various means such as photosynthesis. When an algal cell swims it generally uses a very small amount of its stored energy, so that for any given experiment of several hours duration, or for an overnight interval of active swimming by the cell, energy consumption and supply need not be considered. The supply and consumption time scales are not as well separated for bacteria.

From the Stokes formula one may calculate, for a "typical" algal cell (radius 10 μm, speed 100 μm) a swimming power of 2×10^{-15} J s^{-1} cell^{-1}. The light input can be taken as 1 W m^{-2}; using a photosynthetic conversion efficiency of 3%, and the cell's area, the power input is estimated at 10^{-11} J s^{-1} cell^{-1}. Thus, for algae, swimming requires only a small fraction of the input energy. Estimates for spermatozoan swimming power range from 2×10^{-15} to 2×10^{-13} J s^{-1} cell^{-1} (Bishop 1962); in that case the fluid medium in which they swim can also supply energy. The temperature increase of the fluid due to the swimming power dissipated by a typical cell population is quite negligible. For 10^7 cells cm^{-3}, the temperature rises by 10^{-8} °C s^{-1}. If 1 W m^{-2} light intensity is absorbed and converted to heat by the cells, the temperature rise from that source can be as high as 10^{-4} °C s^{-1}. Illumination can be a source of convection currents in experiments that investigate the interactions of organisms with light.

The doubling time for a bacterial population in exponential growth phase can be as short as 20 minutes. For algae and larger organisms it is generally not less than half a day. Most bioconvection patterns assume

their steady state forms quickly enough for population number changes to be ignored.

2.2 *Dynamics of an Individual Cell*

In general, an individual cell translates and rotates relative to the fluid element in which it finds itself as a result of (*a*) an external body force $\mathbf{F}$ per unit mass, (*b*) an external couple $\mathbf{L}$, and (*c*) intrinsic swimming motions. (*a*) In almost all cases known to us the only relevant body force is gravity [sometimes augmented by placing the cells in a centrifuge (Hemmersbach-Krause & Häder 1990)] which operates whenever the average density $\rho + \Delta\rho$ of the cell differs from ρ of the ambient fluid; in this case $\mathbf{F} = \mathbf{g}\,\Delta\rho/\rho$, where $\mathbf{g}$ is the gravitational acceleration. A cell that is not swimming and for which $\Delta\rho$ is nonzero will have a terminal or sedimentation velocity $\mathbf{V}_t$. (*b*) External couples produce translational motion only for bodies with a particular type of asymmetry such as a helical shape (the same is true for the rotational effect of an external force), and then only if $\mathbf{L}$ has a component parallel to the axis of the helix. Thus even for flagellate swimmers that move their flagella helically, such as bacteria and some spermatozoa, the direct effect of $\mathbf{L}$ on translation can be neglected. (*c*) Different microorganisms exhibit a great variety of swimming motions, mainly using the beating of cilia or flagella to generate a viscous thrust which overcomes the viscous drag on the body and a viscous torque which must be balanced by viscous and external torques on the body (Sleigh 1973, Brennen & Winet 1977). All the cells under consideration, and a fortiori their appendages, move at very small Reynolds number, so inertia can be neglected in modeling the locomotion process (Lighthill 1975, 1976; Childress 1981). The result of the locomotory movements is that a cell has a swimming velocity, $\mathbf{V}_s$, relative to the fluid. In most cases of interest, the magnitude of $\mathbf{V}_s$ is much greater than that of $\mathbf{V}_t$ and sedimentation may be neglected while the cell is swimming. Most cells also rotate as they swim (see Section 2.1 above).

The direction in which a cell swims, represented here by the unit vector $\mathbf{p}$ (so that $\mathbf{V}_s = V_s\mathbf{p}$), is at any instant determined by the balance of viscous and external (in general gravitational) torques on the cell, by internal or external random processes such as rotational Brownian motion (these can be significant but for the purposes of this section will be ignored: see Section 2.4), and by the response of the cell to external influences that elicit directional swimming behavior (light, oxygen concentration, etc.). It will be assumed that such physiological orientation processes can be characterized as equivalent to an external torque which can be added to any other external torques.

There is a fundamental distinction between the external torques which

are actually exerted on a cell, for example by gravity, and the apparent torques which can be used to describe a cell's response to directional sensory information. A locomotory response to a sensory stimulus consists of a change in the beat of the propulsive apparatus so that the cell body turns, moves faster, and so on. Thus, from the viewpoint of a swimming cell, a light beam, say, may seem to exert a turning moment which causes the cell to swim in a direction correlated with the direction of the light beam. It is likely that the combined application of a physical torque and a light beam will result in a motion which can be analyzed by balancing the real and the apparent torque. Initial data on such phenomena (Kessler et al 1991) are encouraging.

At any instant, then, the sum of the total *effective* external torque $\mathbf{L}$ and the viscous torque $\mathbf{L}_v$ exerted by the ambient fluid must be zero. If $\mathbf{L}$ is zero and the cell is not swimming then it will rotate with a time-dependent angular velocity $\boldsymbol{\Omega}$ that depends linearly on the ambient vorticity $\boldsymbol{\omega}$ and strain-rate $\mathbf{E}$, as analyzed for ellipsoidal bodies by Jeffery (1922). If the cell is swimming then the angular velocity is likely to be modified. If $\mathbf{L}$ is nonzero and the ambient fluid at rest, then the cell must either rotate or activate its swimming apparatus to generate an equal and opposite $\mathbf{L}_v$. However, if $\mathbf{L}$ and the ambient velocity gradient are both nonzero, it is possible for the cell to have zero angular velocity or in other words a fixed swimming direction.

Many microorganisms appear to swim, on average, in a given direction, $\mathbf{k}$ say, when the ambient fluid is at rest. This suggests that, if $\mathbf{p}$ were not parallel to $\mathbf{k}$, the body would experience an effective external couple tending to reduce the angle between them. According to the simplest linear model such a couple would have the form

$$\mathbf{L} = L_0 \mathbf{p} \wedge \mathbf{k}. \tag{2.1}$$

Indeed, in the particular example of bottom-heavy spheroidal algae (see above), Equation (2.1) is exactly correct, with $\mathbf{k}$ directed vertically upwards and $L_0 = hmg$, where h is the offset, along the symmetry axis, of the cell's center of mass from its geometric center and m is the cell's mass.

For a general rigid body at zero Reynolds number, the viscous torque $\mathbf{L}_v$ can be written as a linear combination of the velocity and angular velocity of the body relative to the fluid and of the strain rate. For a swimming cell the details of the flagellar or ciliar motions will also be important but their effect on $\mathbf{L}_v$ has as yet been analyzed only for spermatozoa with helically beating flagella in a fluid otherwise at rest (Lighthill 1976). Most of the interesting effects to be discussed can be understood if we treat a cell as a rigid prolate spheroid whose axis of symmetry is aligned with $\mathbf{p}$. In that case,

$$\mathbf{L}_v = \mathbf{Y} \cdot [\tfrac{1}{2}\boldsymbol{\omega} - \boldsymbol{\Omega} + \alpha_0 \mathbf{p} \wedge (\mathbf{E} \cdot \mathbf{p})], \tag{2.2}$$

where

$$\mathbf{Y} = \mu v[\alpha_\parallel \mathbf{pp} + \alpha_\perp (\mathbf{I} - \mathbf{pp})] \tag{2.3}$$

and

$$\alpha_0 = (r^2 - 1)/$$

Here v is the cell volume, r is the ratio of major to minor axis of the cell, and $\alpha_\parallel$, $\alpha_\perp$ are dimensionless constants representing the resistance to cell rotation about axes respectively parallel and perpendicular to $\mathbf{p}$. Since $\mathbf{p}$ is a unit vector, the angular velocity can be written

$$\boldsymbol{\Omega} = \Omega_\parallel \mathbf{p} + \mathbf{p} \wedge \dot{\mathbf{p}}$$

and the vector product with $\mathbf{p}$ of the torque balance equation $\mathbf{L} + \mathbf{L}_v = 0$, with (2.1), gives

$$\dot{\mathbf{p}} = \frac{1}{2B}[\mathbf{k} - (\mathbf{k} \cdot \mathbf{p})\mathbf{p}] + \frac{1}{2}\boldsymbol{\omega} \wedge \mathbf{p} + \alpha_0 \mathbf{p} \cdot \mathbf{E} \cdot (\mathbf{I} - \mathbf{pp}) \tag{2.4}$$

(Leal & Hinch 1972, Hinch & Leal 1972b). (Note that this differs from Equation (1.17) of Pedley & Kessler (1990) by a factor of 2, omitted in error in that paper.) The quantity B in (2.4) is defined by

$$B = \frac{\mu v \alpha_\perp}{2L_0} \tag{2.5}$$

and is a time scale for the reorientation of $\mathbf{p}$ by the external torque against viscous resistance; for the case in which $\mathbf{L}$ is gravitational B was called the "gyrotactic orientation parameter" by Pedley & Kessler (1987). The component of the torque balance equation parallel to $\mathbf{p}$ merely states that the component of the cell's angular velocity in that direction is the same as that of the ambient fluid. That component can be, and in most cases is, modified by swimming motions without affecting Equation (2.4).

2.3 *Effect of the Cells on the Bulk Flow*

Since inertia is negligible in cell swimming the net force and couple on an individual cell is zero. Therefore any external force $\mathbf{F}$ or couple $\mathbf{L}$ on a cell is transmitted to the ambient fluid. If the number of cells per unit volume in a suspension is large, then the aggregate of all the external forces $\mathbf{F}$ may represent a significant body force on the suspension as a whole. This is true even when sedimentation is negligible compared with swimming in determining the cell's velocity; like Brownian motion in a colloid suspen-

sion, the swimming motions do not influence the net force exerted on the suspension as a whole. The effect of this body force is dominant in bioconvection (Section 4).

Similarly the presence of a body couple can have an effect on the motion of the suspension as a whole, by introducing a nonsymmetric contribution $\boldsymbol{\Sigma}^{(L)}$ to the bulk stress tensor $\boldsymbol{\Sigma}$. Here the distinction between actual and apparent external torques is vital: Only actual torques are transmitted to the fluid and provide a body couple to the whole suspension. For example, when a horizontal beam of light shines on a suspension of bottom-heavy algal cells, the cells swim, on average, at an angle to the vertical (Kessler et al 1991). The effective external torque on each cell is (on average) zero, but a net gravitational couple continues to be exerted on the fluid. Incidentally, the sign of $\boldsymbol{\Sigma}^{(L)}$ can be reversed by reversing the direction, or increasing/decreasing the intensity, of the illumination.

Other contributions to $\boldsymbol{\Sigma}$ arise from the fact that a suspended body does not in general deform and rotate in the same way as the fluid would if the body were not there. All these "particle stress" contributions $\boldsymbol{\Sigma}^{(p)}$ were analyzed for suspensions of randomly oriented rigid bodies by Batchelor (1970), in a seminal work that has been the foundation for rational studies of suspension rheology ever since. For a representative suspension of swimming cells, however, Pedley & Kessler (following a suggestion by J. M. Rallison, personal communication) showed that there is another contribution to $\boldsymbol{\Sigma}$, more significant than either $\boldsymbol{\Sigma}^{(p)}$ or $\boldsymbol{\Sigma}^{(L)}$. This arises from the stresslets associated with the organism's swimming motions themselves. For a biflagellate algal cell, the stresslet strength $\mathbf{S}$ was estimated to be

$$\mathbf{S} = 2Tl_1(\mathbf{pp} - \tfrac{1}{3}\mathbf{I}), \tag{2.6}$$

where $2T$ is the drag on the cell body, twice the (viscous) thrust exerted by each flagellum, and l_1 is the distance ahead of the cell center at which, on average, the thrust is applied. Although in the example analyzed by Pedley & Kessler (1990) the contribution $\boldsymbol{\Sigma}^{(s)}$ of these intrinsic stresses was small, it was much bigger than $\boldsymbol{\Sigma}^{(p)}$ and $\boldsymbol{\Sigma}^{(L)}$ and must be considered in future work.

Swimming cells generally rotate while they swim (Section 2.1). Chiral, i.e. rotationally asymmetric, motions of the locomotory organelles produce a torque on the fluid, equal and opposite to that generated by the rotating cell body; the combined effect on the fluid is a "torque-doublet." This is a higher-order flow singularity than the stresslet or the "couplet" associated with an external torque and therefore does not influence the bulk stress tensor.

2.4 *Random Effects*

A population of living organisms exhibits various levels of stochastic behavior. An individual organism in its entirety is subject to thermal fluctuations which result in Brownian motion. In the cases considered here, translational Brownian motion is negligible compared with swimming, but rotational Brownian motion could be an important determinant of swimming direction (Berg 1983). For a bottom-heavy organism whose center of mass is offset by a distance h relative to the center of buoyancy, the criterion for deciding on the relative strengths of gravitational alignment and rotational diffusion involves mgh/kT, where m is the mass of the organism, g is the acceleration of gravity, and kT is the thermal energy. For algae such as *Chlamydomonas* this parameter is around 100 showing that Brownian rotations are negligible. For geometrically similar 2-μm bacteria it would be about 0.16, and even smaller if the mass distribution were less asymmetric, so Brownian rotations could be important (Kessler 1990). In fact, however, the orientation of bacteria is dominated by other influences (e.g. chemotaxis), and Brownian rotations are again unimportant.

The foregoing comments apply to a precisely built mechanical automaton as well as to a biological cell. The latter may exhibit stochastic, seemingly or actually capricious, behavior which might be relatable to fluctuations in chemical concentration or light intensity of the environment, or to thermally generated fluctuations within the locomotory apparatus of the cell itself. Kawakubo & Tsuchiya (1981) suggested membrane fluctuations as one possibility. A convenient way to model such biological stochastic behavior is to subsume it into an effective "kT" factor, leading to an effective rotational diffusivity (Pedley & Kessler 1990). Eventually it should be possible to validate this procedure, by the results obtained, and by computer-assisted statistical analysis of many cell trajectories.

There exist additional fluctuations which are actually stochastic or can be modeled as if they were. Cell concentration is one of these, where mixing processes presumably cause it to fluctuate by $\sqrt{N}/N$, where N is the cell number in a particular volume. Such fluctuations can be involved in the initiation of plumes and bioconvection patterns (see Section 4). Cell size and behavior are also subject to fluctuations. The principal causes of this polydispersivity are the distribution of cell ages within a culture and imperfections in cell replication. Secondary fluctuations also occur. These can be due to shading of some individuals by the rest of the population, or to the effect of a fluctuating concentration of population members on local chemical concentrations seen by a particular cell. It is no surprise that polydispersivity of a cell population can convert a sharply peaked,

calculated distribution of deterministically guided cells into a broad, nearly Gaussian one (see Section 3.2). Presumably, if one incorporates sufficiently many stochastic processes, the central limit theorem will permit relatively simple parameterization of the entire collection—possibly into an effective kT.

3. BEHAVIOR IN A PRESCRIBED FLOW

3.1 *Individual Orientations and Trajectories*

In the absence of random effects, Equation (2.4) can be used to determine a cell's swimming direction $\mathbf{p}$ as a function of time for any set of initial conditions. In many situations, however, the solution tends to a stable equilibrium value $\mathbf{P}$, in a time of order B. In those cases, if the time-scale for the variation of $\boldsymbol{\omega}$ and $\mathbf{E}$, or the time required for the cell to swim to a location where $\boldsymbol{\omega}$ and $\mathbf{E}$ are different (R/V_s, where R is a length scale for the flow), is large compared with B, then the cell trajectory can be calculated by setting $\mathbf{p}$ equal to $\mathbf{P}$ at all times. If a stable equilibrium orientation does not exist, $\mathbf{p}$ will follow an orbit in the two-dimensional $\mathbf{p}$-space (the unit sphere), as calculated by Jeffery (1922) for zero external couple ($B = \infty$).

The first calculation of orientation for particles with an external couple of the form (2.1) was made by Hall & Buesenberg (1969) (their application was to magnetized particles in a uniform magnetic field parallel to $\mathbf{k}$). These authors considered spherical particles, so that $\alpha_0 = 0$ and strain-rate would have no effect on $\mathbf{p}$, and showed that there is a unique, stable, equilibrium orientation $\mathbf{P}$ unless both $\boldsymbol{\omega}\cdot\mathbf{k} = 0$ and $B\omega > 1$, where $\omega = |\boldsymbol{\omega}|$. In that case $\mathbf{p}$ performs a periodic orbit with period $2\pi B(B^2\omega^2 - 1)^{-1/2}$. If we think of $\mathbf{k}$ as being vertically upwards, as for bottom-heavy algae, the case $\boldsymbol{\omega}\cdot\mathbf{k} = 0$ corresponds to a flow whose vorticity is entirely horizontal, such as unidirectional flow in a vertical pipe. Many experimental investigations have employed flows of this nature. In this case, when $B\omega < 1$, the orientation of $\mathbf{P}$ is given by

$$\sin\theta = B\omega, \quad \cos\theta > 0, \quad \sin\phi = -\omega_1/\omega, \quad \cos\phi = \omega_2/ \tag{3.1}$$

where (θ, ϕ) are spherical polar angles with $\theta = 0$ parallel to $\mathbf{k}$, the 3-axis, and $\phi = 0$ being the vertical 1–3 plane, containing the origin of coordinates and the cell center (see Pedley & Kessler 1987).

For Poiseuille flow in a vertical circular pipe, this means that gyrotactic algal cells swim upwards (relative to the flow) and in towards the axis ($\phi = \pi$) for downflow, out towards the walls ($\phi = 0$) for upflow, as long as $B\omega$ remains less than 1. Indeed, it was the observation that swimming algal cells became focussed on the axis of a downwards pipe flow (and

migrated to the walls in upflow) that confirmed the hypothesis of bottom-heaviness, leading to gyrotaxis (Kessler 1985a; see Section 3.2).

When a small vertical component of vorticity is present the stable equilibrium orientation **P** is not greatly altered from that given by (3.1) as long as $B\omega < 1$. When $B\omega > 1$, however, the stable equilibrium becomes one in which $\sin\theta \approx 1$ and the cells tend to spiral in towards the axis, swimming in a horizontal plane relative to the fluid. When $B\omega \gg 1$, a cell's trajectory becomes almost circular, the radially inwards component of velocity being very small (Pedley & Kessler 1987).

For nonspherical cells the orientation depends on both the vorticity and the strain rate in the ambient flow (Equation 2.4). A variety of simple flow fields, symmetric about a vertical axis or two-dimensional in a vertical plane, have been considered by Pedley & Kessler (1987), and the results can be roughly summarized as follows. For flows in which the vorticity and the strain-rate are comparable (vertical pipe flow or simple shear flow) there is one stable equilibrium orientation if $B\omega$ is less than a certain critical value and none if $B\omega$ exceeds that value; periodic orbits then presumably exist. For pure straining flows (conical sink flow, two-dimensional stagnation-point flow) there is one stable equilibrium orientation for values of BE (E is a characteristic strain rate) less than a certain critical value, but there are *two* stable equilibria for larger values of BE. In each case the critical value of the flow parameter depends on α_0 and the precise orientation of the flow. Calculations have not been made for flows with a nonzero vorticity that is small compared with the strain rate. Observations of cell populations in which two stable orientations are predicted have not yet been made, nor have the implications of this result been worked out. Observations have been made of algae in a simple shear flow and observed cell trajectories agree qualitatively with the predictions, as for pipe flow (Kessler, unpublished).

Further interesting predictions were made for gyrotactic cells swimming in the far field of a dense sphere falling through the fluid at low Reynolds number. More rounded cells ($\alpha_0 < \frac{1}{3}$) would be focussed into the wake of such a sphere, while elongated cells ($\alpha_0 > \frac{1}{3}$) would swim away from the wake. Since the far field of such a sphere depends only on the net force it exerts on the fluid, the same focussing (or anti-focussing) would occur if it were itself swimming upwards. This gives a potential, but as yet unconfirmed, mechanism for the efficient predation of populations of swimming algae by larger organisms. Incidentally, the elongated cells would not necessarily escape, since below the larger sphere they are focussed inwards, while the rounded ones swim away.

Timm & Okubo (1991) have made an interesting extension to the above predictions of gyrotaxis in the flow field of a falling sphere by computing

the trajectories of spherical cells ($\alpha_0 = 0$) from initial locations ahead of the sphere and at arbitrary distances from the axis of symmetry. They deem an algal cell to be captured if its trajectory brings it sufficiently close to the falling sphere, and they can thus compute the "capture cross-section" of the falling sphere. The calculation is complicated by the fact that for certain values of BW_0/a (where W_0 and a are the velocity and radius of the falling sphere) there exists a critical zone near the sphere in which $B\omega > 1$ so there is no equilibrium orientation (3.1); in that case (2.4) must be integrated numerically for each relevant trajectory (the integration is simplified by the fact that $\theta = \pi/2$ at the point where the trajectory enters the critical zone).

In a steady but nonuniform velocity field, a cell's orientation will change gradually with time—assuming that a stable equilibrium orientation exists for each spatial location—because as it swims the cell's trajectory will take it to different locations where the vorticity and strain rate are different. Computations of the trajectories of individual cells, still neglecting random effects, have been made for spherical cells ($\alpha_0 = 0$) in downwards pipe flow by Kessler (1986a). If the vertical velocity of the fluid is

$$w(r) = -W_0\left(1 - \frac{r^2}{R^2}\right), \tag{3.2a}$$

where r is the radial coordinate (horizontal), R is the radius of the pipe, and $W_0/2$

$$\omega_1 = -\omega_2 = 2W_0 r/R^2, \qquad \omega_3 = 0. \tag{3.2b}$$

Thus, as long as $B\omega < 1$ for all $r \leq R$,

$$\mathbf{p} = [-B\omega, 0, (1 - B^2\omega^2)^{1/2}], \tag{3.2c}$$

from (3.1), and the equation of the trajectory is

$$\frac{dr}{dt} = -BV_s \frac{2W_0 r}{R^2}\left(1 - \frac{r^2}{R^2} - \frac{1}{W_0}\left(1 - 4B^2W_0^2\frac{r^2}{R^2}\right)^{1/2}\right], \tag{3.3a}$$

$$\frac{2BV_s}{R^2}\frac{dz}{dr} = \frac{z}{r}\left(1 - \frac{r^2}{R^2} - \frac{1}{W_0}\left(1 - 4B^2W_0^2\frac{r^2}{R^2}\right)^{1/2}\right], \tag{3.3b}$$

where z is the axial coordinate, measured upwards. The factor BV_s called β by Kessler (1986a); it denotes the distance swum by a cell in one orientation time, about 0.21 mm for an algal cell with $B = 3.4$ s, $V_s = 63$ μm s^{-1}. Equations (3.3) are easy to integrate for arbitrary initial position (r_0, z_0). It is clear that, if V_s/W_0

V_s/W_0

wall, downwards; every trajectory eventually asymptotically approaches the tube axis.

Similar trajectory calculations have been made for a simple shear flow in a vertical plane (Kessler 1986a), which is also experimentally realizable. Using the coordinate system depicted in Figure 1, the trajectory equations are given by

$$\frac{dx}{dt} = Sy + V_s \sin(\psi + \theta), \qquad \frac{dy}{dt} = V_s \cos(\psi + \theta), \tag{3.4}$$

where S is the imposed shear rate and ψ is the angle the streamlines make with the horizontal. For spherical cells the gyrotaxis angle θ is given by

$$\sin\theta = BS$$

from Equation (3.1), as long as $BS < 1$. For spheroidal cells θ is given by

$$\sin\theta = BS[1 + \alpha_0 \cos(2\theta + 2\psi)]$$

and exists as long as BS is less than a critical value depending on α_0 and ψ (Pedley & Kessler 1987). We may note from (3.4) that even gyrotactic cells are predicted to follow the streamlines if $\psi + \theta = \pi/2$. This has not yet been tested experimentally, although observations with $\psi = \pi/2$ show qualitative agreement with (3.4) (Kessler, unpublished).

The particular microorganism chosen to illustrate the above discussion has been that of the bottom-heavy, gyrotactic, spherical or spheroidal algal cell for which **k** is vertically upwards and the viscous torque is given by (2.2). Such an organism is propelled by beating flagella at the front or top

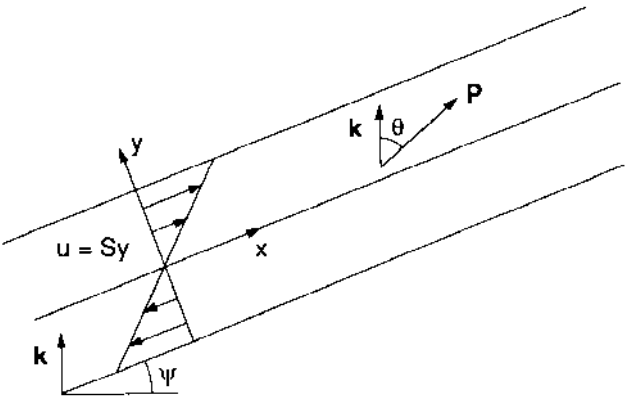

Figure 1 A shear flow $u = Sy$ inclined at an angle ψ to the horizontal; the deterministic swimming direction **P** makes an angle θ with the vertical (**k**).

end, but the effect of the flagella on the torque has been neglected. Similar considerations presumably apply to bacteria, propelled by rotating flagella, except that **k** will be related to the chemotactic gradient, and the cells are much smaller so that their trajectories may be expected to exhibit greater randomness.

However, there is one class of microorganism which has been extensively studied and which requires separate consideration: spermatozoa. These usually have a single tail flagellum, but it is so much longer than the head (e.g. 45 μm compared with 10 μm for bull sperm) that it is not accurate to treat the whole swimming cell as a rigid spheroid (Katz & Pedrotti 1977), although an inert cell can be thought of as an elongated body. In this case the center of mass is located in or near the head, so **k** is directed vertically downwards. Observations by Bretherton & Rothschild (1961) on spermatozoa in a horizontal flow between two microscope slides show that dead cells have their heads pointing downstream in the top half of the flow and upstream in the bottom half, as would be predicted by the torque balance corresponding to (3.1). After sedimentation has acted for some time, then, most dead cells appear to point upstream. Live spermatozoa were recorded by the same authors as pointing upstream,[1] on average, in both halves of the flow; no explanation for this curious result was offered. Roberts (1970) also observed upstream orientation to be dominant in a horizontal tube flow, and supposed that the cells exhibiting the effect were in the lower half, having tended to swim downwards, in accordance with (3.1), much more quickly than sedimentation would account for. Winet et al (1984), however, made careful observations of human sperm in both horizontally and vertically oriented glass flow channels and found no difference in either the distribution of cells with distance y from the wall, or the distribution of mean swimming direction with y, no matter whether the wall was a top wall, a bottom wall, or a vertical wall. Indeed most cells tended to swim upstream, but that was a consequence of swimming towards the wall and being correspondingly rotated by the shear. The tendency to approach the wall was very much greater than the tendency to swim downwards. In each case, the majority of the cells were to be found within 100 μm of the wall, with a maximum concentration at $y \approx 10$ μm. We have found no explanation in the literature for the accumulation of spermatozoa near boundaries, though we may note that if the time required for a cell to change its swimming direction were significantly

[1] We have avoided the terms *positive rheotaxis* and *negative rheotaxis* because conventions differ. Bretherton & Rothschild (1961) and Roberts (1970, 1975) describe upstream swimming as positive rheotaxis, while Winet et al (1984) describe it as negative rheotaxis. The term rheotaxis was originally coined to describe the tendency for fish to point their heads upstream in a rapid flow (Fraenkel & Gunn 1940).

longer than the time to swim across the channel, then such accumulation would inevitably follow. The importance of these results in reproductive physiology is likely to be considerable.

3.2 *Focusing of Trajectories*

The behavior of individual microorganisms can be observed only through a microscope, but aspects of their behavior can be inferred from observations on the laboratory scale of large numbers of them in suspension. High cell concentrations can be easily seen. For example, Kessler (1985a,b, 1986a,b) has used algal cells of the genera *Dunaliella* and *Chlamydomonas* in his experiments. These have a mean diameter d in the range 10–2
Assuming that $d = 15$ μm and that cell concentration n ranges between 10^4 and 10^7 cells cm^{-3}, one may estimate the mean free path for light absorption, $\lambda \approx 4/\pi n d^2$
centration looks very dark green compared with the low concentration. Even at the high end of this concentration range, however, the suspension is still dilute, the volume fraction being about 0.02.

Motile algal cells in still water tend to swim upwards as discussed above (Section 2.
of this statement is inferred from the fact that when a suspension of the algae is placed in a vertical pipe and a through-flow is imposed, the swimming cells concentrate themselves in a green core on the axis for downflow and in sheets at the walls for upflow (Kessler 1985a,b). This phenomenon is predicted by the above theory of cell orientation and cannot be explained by any other realistic mechanism. Dead cells are not concentrated. In this and the next two sections we examine analyses of the distribution of cell concentration in the focussed core in downflow. These may be compared qualitatively with the concentration distribution measured by Kessler (1985b) from photographic negatives using an optical densitometer.

One way of working out the concentration distribution is to assume a uniform concentration n_0
and integrate the trajectory Equation (3.3b) for arbitrary initial radius r_0. After an initial transient, the concentration $n(r, z)$ at a lower level, z, will be time-independent and can be calculated from conservation of cells in the annulus between the trajectories through (r_0, z_0) and $(r_0 + dr_0, z_0)$. This shows that nr^2 is conserved on a trajectory. If it is assumed that V_s
then a typical trajectory is given by

$$\frac{4BV_s}{R^2}(z_0 - z) = 21 \qquad \frac{1}{} \quad 2 \quad 2 \tag{3.5}$$

and $n(r, z)$ is given by

$$\frac{4BV_s}{R^2}(z_0-z) = \log\frac{n}{n_0} + \frac{r^2}{R^2}(1-n/n_0) \tag{3.6}$$

(Kessler 1985b). This expression is valid within the trajectory that originates at (R, z_0); outside that trajectory $n = 0$. There is a concentration defect on the axis relative to the maximum. Neither this defect nor the sharp cutoff from maximum concentration to zero at the outer trajectory is observed experimentally.

The source of the discrepancy lies in the fact that in practice the cells (*a*) are not identical and (*b*) do not behave deterministically, i.e. they have a random component contributing to their orientation at any time (Section 2.4). The former can be accounted for by incorporating a distribution of values of the gyrotactic length scale BV_s, which succeeds in smoothing the sharp cutoff but cannot eliminate a dip on the axis (though a sufficiently wide spread of BV_s would make the dip virtually impossible to observe). The latter could be included by a Monte Carlo calculation, but this has not been done. However, the standard theories of stochastic processes suggest that the macroscopic effect of the random aspects of cells' behavior can, to a first approximation, be modeled as diffusion.

3.3 *Cell Conservation*

From now on we model the suspension as a continuum, of which each fluid element contains large numbers of cells, n per unit volume, which in general swim in random directions $\mathbf{p}$; $\mathbf{p}$ is taken to be a stationary random variable with probability density function (p.d.f.) $f(\mathbf{p})$. Neglecting sedimentation the equation describing the conservation of cells is

$$\frac{\partial n}{\partial t} = -\nabla\cdot[n(\mathbf{u}+\mathbf{V}_c) - \mathbf{D}\cdot\nabla n], \tag{3.7}$$

where $\mathbf{u}$ is the bulk fluid velocity (supposed given in this section), $\mathbf{V}_c$ is the average cell swimming velocity and $\mathbf{D}$ is the cell diffusivity tensor. Defining $\langle\cdots\rangle$ as the ensemble average, given for functions of $\mathbf{p}$ by

$$\langle\cdots\rangle = \iint\cdots f(\mathbf{p})d^2\mathbf{p},$$

where the integral is over the surface of the unit sphere in $\mathbf{p}$-space, we may write

$$\mathbf{V}_c = \langle V_s\mathbf{p}\rangle = \langle V_s\rangle\langle\mathbf{p}\rangle, \tag{3.8}$$

the latter expression being valid if V_s, the swimming speed, is a stationary random variable independent of $\mathbf{p}$. The diffusivity tensor is given by

$$\mathbf{D}(t) = \int_0^{\infty} \langle \mathbf{V}_r(t)\mathbf{V}_r(t-t')\rangle \, dt',$$

where $\mathbf{V}_r$ is the velocity of a cell relative to $\mathbf{V}_c$, so in the special case where V_s

$$\mathbf{D} = V_s^2 \tau \langle (\mathbf{p} - \langle \mathbf{p} \rangle)(\mathbf{p} - \langle \mathbf{p} \rangle)\rangle, \tag{3.9}$$

where τ is the direction correlation time. This is the form used by Pedley & Kessler (1990).

The deterministic description of cell focusing in pipe flow given in Section 3.2 can be obtained from (3.9) by setting $\mathbf{D} = 0$ and $\mathbf{V}_c = V_s\mathbf{P}$, where $\mathbf{P}$ is the stable gyrotactic swimming direction, if it exists, given by (3.1). With diffusion present, (3.7) has been solved in the case where n is a function of the radial coordinate r only, as expected sufficiently far from the inlet. In that case, with the fluid velocity $w(r)$ also independent of z, the advective term drops out of (3.7), leaving a balance between radial inswimming and outwards diffusion. A single integration (using the boundary condition $\partial n/\partial r = 0$ at $r = 0$) gives

$$D_{rr}\frac{dn}{dr} = nV_{cr}. \tag{3.10}$$

Kessler (1985b, 1986a,b) has given the solution to this equation when V_{cr} (the radial component of the average cell swimming velocity) is given by (3.1) to be

$$V_{cr} = -BV_s\frac{dw}{dr}, \tag{3.11}$$

and for a constant radial diffusivity D_{rr}. The solution is

$$n = n(0)\exp\left\{-\frac{BV_s}{D_{rr}}[w(r) - w(0)]\right\}, \tag{3.12a}$$

where $n(0)$ should be determined by global cell conservation, i.e.

$$2\pi\int_0^R n(r)\, dr = \pi R^2 N_0, \tag{3.13}$$

N_0 being the given average concentration in the suspension as a whole.

For Poiseuille flow (3.2a) we have

$$n = n(0)\, e^{-kr^2/R^2} \tag{3.12b}$$

where $k = BV_sW_0$

consistent with qualitative experimental results obtained by collecting the focussed cells in a three-segment collector. However, D_{rr} is unlikely to remain a constant, for one thing because of cell-cell interactions: The ability of the cells to move about randomly will be restricted in regions of high cell concentration. Kessler (1986a) gave a simple model for this collisional diffusion process. Moreover, even for a sufficiently dilute suspension in which cell-cell interactions can be neglected it is questionable whether (3.10) can be used with (3.11). The latter assumes that the cell swimming direction is always equal to its deterministic value $\mathbf{P}$, so randomness is negligible, while the incorporation of diffusion explicitly recognizes that randomness is important. Another problem is that at sufficiently large radius the vorticity will become so large that $B\omega > 1$ so no stable swimming direction exists. What is required is a rational model for the orientation p.d.f., $f(\mathbf{p})$, which will allow nondeterministic estimates to be made for $\mathbf{V}_c$ and $\mathbf{D}$, from Equations (3.8) and (3.9). This procedure ought to yield results analogous to the statistical mechanical Einstein relation between mobility and diffusivity.

3.4 *The Fokker-Planck Equation*

Such a model was provided by Pedley & Kessler (1990). It was assumed that, in the absence of all torques, the cells swim in totally random directions, with an isotropic p.d.f., $f = 1/4\pi$, and an isotropic diffusivity $\mathbf{D} = \frac{1}{3}V_s^2\tau\mathbf{I}$. In the presence of viscous and gravitational torques, however, the p.d.f. will be biased by the tendency for $\mathbf{p}$ to approach $\mathbf{P}$ after every random change of direction. Assuming that the intrinsic tendency for the cells to change direction randomly is independent of the instantaneous direction, we may model the process as analogous to that of colloidal particles in suspension under the action of rotatory Brownian motion, for which there is already much theory [e.g. Brenner (1974), Hinch & Leal (1972a), etc.]. We therefore assert that $f(\mathbf{p})$ must satisfy the Fokker-Planck equation

$$\frac{\partial f}{\partial t} + \nabla \cdot (\dot{\mathbf{p}} f) = D_r \nabla^2 f, \tag{3.14}$$

where ∇ is the gradient operator in $\mathbf{p}$-space, $\dot{\mathbf{p}}$ is the deterministic reorientation rate given by (2.4), and D_r is a rotational diffusivity, taken for simplicity to be isotropic and constant. The effect of other cells on the orientation of a particular cell is neglected, which means that the model can be valid only for sufficiently dilute suspensions. A further assumption is that the $\partial f/\partial t$ term can be neglected in (3.14), which requires the time scale for unsteadiness in the flow to be large compared with D_r^{-1}. We also, for convenience, continue to assume that V_s is a given constant, not a random variable, though its randomness would affect (3.9).

In the case of zero ambient flow, only the first, gravitational term remains on the right hand side of (2.4). The solution of (3.14) is then axisymmetric and takes the form

$$f = \frac{\lambda e^{\lambda \mathbf{k}\cdot\mathbf{p}}}{4\pi \sinh \lambda}, \tag{3.15}$$

(Brenner & Weissman 1972) where

$$\lambda = (2BD_r)^{-1}: \tag{3.16}$$

small λ means that randomness dominates and f is almost isotropic, while large λ means that reorientation by the torque balance dominates so f is almost proportional to $\delta(\mathbf{p}-\mathbf{P})$. When f is given by (3.15), $\mathbf{V}_c$ and $\mathbf{D}$ can be readily calculated. $\mathbf{V}_c$ is vertical, with

$$V_c/V_s = \coth \lambda - 1/\lambda \equiv K_1;$$

$\mathbf{D}$ is diagonal and axisymmetric, and the ratio of the horizontal to vertical diffusivities is

$$\frac{D_H}{D_V} = \frac{K_1}{\lambda K_2} > 1, \quad \text{where} \quad K_2 = 1 - \coth^2 \lambda + 1/\lambda^2.$$

These results, used together with preliminary data from measured trajectories of individual cells of *C. nivalis* (Häder & Hill 1991), gave an estimated value for $\lambda \approx 2.2$ for that species. Combined with $B = 3.4$ s (Pedley et al 1988) this gives an estimate for D_r, from (3.16), of 0.067 s^{-1}. [This is a factor 2 lower than the value given by Pedley & Kessler (1990) because of the factor 2 missing from Equation (2.4).] For comparison the thermal rotational diffusion coefficient for a 10-μm diameter sphere is 1.3×10^{-3} s^{-1}.

Pedley & Kessler (1990) also computed the first-order correction to (3.15) for a weak ambient flow, i.e. for small values of the parameter

$$\varepsilon = B\omega, \tag{3.17}$$

where here ω is used as a scale for the ambient velocity gradient. For the case of spherical cells in downwards pipe flow we use cylindrical polar coordinates (r, ϕ, z), so the z-velocity is given by (3.2a), the vorticity by (3.2b), and $\varepsilon = 2BW_0 r/R^2$. The results of the theory give

$$\frac{\mathbf{V}_c}{V_s} = \langle \mathbf{p} \rangle = (-\varepsilon J_1, 0, K_1),$$

where J_1 is another function of λ defined by Pedley & Kessler (1990)

(when $\lambda = 2.2$, $K_1 \approx 0.57$, $J_1 \approx 0.45$); note that this is not parallel to $\mathbf{P} = (-\varepsilon, 0, 1)$. The diffusivity tensor is given by

$$\frac{\mathbf{D}}{V_s^2\tau} = \begin{pmatrix} K_1/\lambda & 0 & \varepsilon(J_2 - K_1J_1) \\ 0 & K_1/\lambda & 0 \\ -\varepsilon(J_2 - K_1J_1) & 0 & K_2 \end{pmatrix}$$

where $J_2(\lambda) \approx 0.16$ when $\lambda = 2.2$. The solution of the cell conservation Equation (3.10) for a z-independent distribution is again (3.12b), but with $k = (\lambda J_1/K_1)(BW_0/\tau V_s)$; this indeed represents a narrow, concentrated core down the tube axis as long as $k \gg 1$. Using the estimates given by Pedley & Kessler (1990), this requires $W_0 \gg 0.22V_s \approx 14\ \mu\text{m s}^{-1}$; in his published experiments Kessler used centerline velocities of 1–3 mm s^{-1}.

Since ε is proportional to r, the above solution will always be valid sufficiently close to the axis. It will therefore be valid wherever there is a substantial cell concentration if ε is still small at $r = 2k^{-1/2}R$, say, i.e. if $4(K_1/\lambda J_1)^{1/2}(BW_0\tau V_s/R^2)^{1/2} \ll 1$. For *C. nivalis* in a 1-cm radius tube with $W_0 = 1\ \text{mm s}^{-1}$, this quantity is approximately 0.28, so the solution should be reasonably accurate. However, for larger velocities, ε will not be small throughout the concentrated core and (3.12b) will not be a good approximation to $n(r)$. The theory for general values of ε can be derived by extending the analysis of Brenner & Weissman (1972) on dipolar spherical particles undergoing Brownian rotations. In particular, an analytical solution is available at large values of ε, for which the torque due to the ambient vorticity is much greater than the gravitational torque, so that no stable equilibrium orientation $\mathbf{P}$ exists even in the absence of randomness. The results, up to $\mathcal{O}(\varepsilon^{-2})$, are

$$\langle \mathbf{p} \rangle = \frac{2}{3\varepsilon}\left(-1, 0, \frac{2}{\lambda\varepsilon}\right)$$

$$\frac{\mathbf{D}}{V_s^2\tau} = \frac{1}{3}\begin{pmatrix} 1 - \dfrac{9}{15\varepsilon^2} & 0 & 0 \\ 0 & 1 - \dfrac{4}{15\varepsilon^2} & -\dfrac{4}{\varepsilon^2} \\ 0 & -\dfrac{4}{\varepsilon^2} & 1 - \dfrac{7}{15\varepsilon^2} \end{pmatrix}$$

(Pedley, unpublished). In this case the solution to (3.10) is

$$n = N_1\left(\frac{r^2}{R^2} \quad \frac{9R^2}{60B^2W_0^2}\right)^{-\chi}, \tag{3.18}$$

where $\chi = R^2/(2BW_0\tau V_s)$ and N_1 is a constant, which will be determined in terms of the centerline concentration $n(0)$ by matching this solution to (3.12b) in an intermediate zone. Clearly the outer solution (3.18) is valid only for $r \gg R^2/BW_0$ ($\varepsilon \gg 1$). The algebraic falloff with radius in (3.18) is much more gradual than the exponential decay of (3.12b). This is a consequence of the much weaker tendency to swim inwards, and the diffusivity tensor becoming more isotropic, when the random intrinsic reorientations are acting on a deterministic orientation which itself varies on a periodic orbit (cf Leal & Hinch 1971).

In summary then, the explicit recognition from the start that there is a random distribution of cell orientations, whose p.d.f. satisfies the Fokker-Planck equation, enables a rational theory of microorganism suspensions to be developed, whatever the strength of the ambient flow and whatever external torques are acting on the cells. Such a theory should be the basis of future studies of collective behavior in such suspensions. In general, for spheroidal or more complicated cells, and for flows of arbitrary strength, the Fokker-Planck equation will have to be solved numerically, guided by the above and other analytical solutions (e.g. Leal & Hinch 1971, 1972; Hinch & Leal 1972a,b).

3.5 *Instability of a Focussed Beam*

The focussed beam of algae in a downwards pipe flow experiment is often observed to develop an instability in the form of regularly-spaced, axisymmetric blips, (Kessler 1985b, 1986b). The blips are regions of increased cell concentration, which become roughly spherical with a visible radius two or three times that of the beam; they fall at a faster velocity than the imposed centerline velocity W_0 and therefore have an internal vortex-ring structure. Blips tend to form more readily for larger values of the initial, uniform cell concentration N_0 or for smaller values of W_0. Of course, once the blips have formed the velocity field is no longer given by the imposed Poiseuille flow, but the breakdown of that flow properly forms a part of this section.

The reason that blips fall faster than their surroundings lies in the fact that the algal cells are denser than water ($\Delta\rho/\rho \approx 0.05$): A drop of fluid containing more cells than its surroundings thus must fall relative to its surroundings. This also means that the focussed beam itself will have a velocity greater than W_0, an effect which we have neglected hitherto on the grounds that the difference would be small. However, the details of the velocity profile, in particular the presence of inflection points, may be crucial in the instability mechanism.

The z-independent axial velocity profile in the presence of negative cell buoyancy is given by the momentum equation

$$\frac{1}{r}\frac{d}{dr}\left(r\frac{dw}{dr}\right) = \alpha n + p_z/\mu, \tag{3.19}$$

where $\alpha = vg\Delta\rho/\mu$, μ is the fluid viscosity, and p_z is the uniform imposed pressure gradient (recall that z is measured upwards, $w < 0$ and $p_z > 0$ for imposed downflow). Assuming that W_0 is small enough for the small-ε solution of the Fokker-Planck equation to be valid, the cell-conservation Equation (3.10) again has the solution (3.12a), with V_s replaced by $J_1 V_s$. When combined with (3.19) this results in a nonlinear ordinary differential equation for w (or n) for which a general solution cannot be written down (see Joseph & Lundgren 1973, Childress & Percus 1981). However it is clear that if p_z (and hence W_0) is big enough there is no inflection point in the profile, but that there does exist an inflection point for sufficiently small p_z. In particular, when $p_z = 0$ a solution satisfying the boundary conditions is

$$n(r) = \frac{n(0)}{(1+\gamma n(0) r^2)^2}, \tag{3.20}$$

where $\gamma = \alpha J_1 B V_s/8D_{rr}$; the corresponding velocity profile has an inflection point at $r = [\gamma n(0)]^{-1/2}$. This solution corresponds to a plume that can form spontaneously in a tube with no ends and no imposed flow, but it may not be realized in practice because global cell conservation (3.13) shows that $n(0) = N_0/(1-\gamma N_0 R^2)$, which becomes infinite if either N_0 or R is too big. Kessler (1986b) speculated that a possible reason for the formation of blips could be the nonexistence of a corresponding steady solution. The result also has implications for the spacing of spontaneously formed plumes in a wide chamber (see Section 4.4).

What are the possible instability mechanisms when a steady state does exist? Blip instabilities are also observed on thin columns of dense dye falling longitudinally in an otherwise still fluid, so the swimming of the cells is not a necessary condition for instability. At least two possible mechanisms appear to exist. First, if a somewhat wider or more concentrated blob forms on the column it will tend to fall more rapidly than the rest of the column and will entrain more dense fluid from the column as it falls, enhancing both its size and its speed of fall. This mechanism will actually lead to instability unless the corresponding perturbation to the viscous stresses is such as to prevent it; it does not require a high Reynolds number. Second, when the velocity profile has an inflection point it is much more prone to suffer a shear instability, independently of the density distribution, but only at fairly high Reynolds number. The two mechanisms may of course both be destabilizing. There is apparently no

way that cell swimming can have a qualitatively distinct effect, but it will make a quantitative difference to the growth rate of the blips as a result of both gyrotaxis and cell diffusion.

A relevant theory is that of Smith (1989), who analyzed the stability of a vertical column of one fluid on the axis of a cylinder containing another, both acted upon by a uniform pressure gradient. The densities of the two fluids were different but their viscosities were the same. Interdiffusion of the two fluids was ignored, but most of the discussion concerned the case of zero surface tension. The analysis was limited to long axial wavelengths, and the Reynolds number remained of $\mathcal{O}(1)$ in that limit so that shear instabilities were ruled out. For the case in which the inner fluid was slightly denser, Smith found instability if the downwards pressure gradient dp/dz exceeds a certain critical value, which depends on the radius ratio. The mechanism of the instability relied on a rather subtle interaction between the perturbations to the viscous shear stress and the pressure, but is presumably allied to the first of those outlined above. The critical pressure gradient can be negative, leading to upflow in the outer region, but in general the more vigorous the downflow the more unstable the flow. This is contrary to the few observations (Kessler 1986b) that indicate a greater propensity to instability if the downflow is decelerated; further theoretical and experimental work is clearly desirable.

4. BIOCONVECTION

4.1 *Observations*

Bioconvection is the name given to the process of spontaneous pattern formation in suspensions of upswimming microorganisms. The name was apparently coined in 1961 (Platt 1961) but the patterns have been known since at least 1848 (see Wager 1911). Patterns have been seen in suspensions of ciliated protozoa, especially *Tetrahymena pyriformis* (Loeffer & Mefferd 1952, Platt 1961, Winet & Jahn 1972, Levandowsky et al 1975), spermatozoa (Rothschild 1949), bacteria (Wager 1911, Nettleton et al 1953, Pfennig 1962, Spormann 1987, Kessler 1989), dinoflagellates (Levandowsky et al 1975), and flagellated green algae from genera such as *Chlamydomonas*, *Dunaliella*, *Euglena*, and *Volvox* (Wager 1911, Brinkmann 1968, Nultsch & Hoff 1973, Kessler, 1984b, 1985b, 1986a). In the case of magnetotactic bacteria (Spormann 1987), the bacteria swim along magnetic field lines, and waves of concentration are generated with crests more or less perpendicular to the field lines. In the case of spermatozoa (Rothschild 1949), wavelike concentrations of cells were reported as evidence of large-scale motions but were not described in detail. We will not refer to these cases as bioconvection because upswimming is not involved.

In all other cases of pattern formation, however, the following features are found: The cells are denser than the medium they swim in, they tend to swim upwards, on average, in still water, and the patterns die away if the cells stop swimming. The cause of the upswimming orientation is not the same in each case (gravity-sensing, bottom-heaviness, chemotaxis, phototaxis), but the patterns show great similarities between different species and orientation mechanisms.

When bioconvection takes place in a shallow chamber (<1 cm deep) the pattern may be observed from above, because falling regions of high cell concentration absorb or reflect light differently from their surroundings. The patterns take a variety of forms (Figure 2): a regular, often square, array of dots, each a concentrated plume (Wager 1911, Winet & Jahn 1972, Kessler 1985b, 1986a) (Figure 2*a*); a regular, square or hexagonal, array of lines or "filaments" representing falling sheets of cells, which are often a transitory phase on the way to an array of dots (Wager 1911, Winet & Jahn 1972, Kessler 1986a, 1989) (Figure 2*b*)—there is evidence that the branching pattern of these filaments may have a fractal structure (Noever 1990a); a "labyrinthine" structure of banded rolls, with some hexagonal features (Wager 1911, Levandowsky et al 1975) (Figure 2*c*).

The nature and the size of the patterns are influenced by a number of variables. Principal among these are the average cell concentration N_0 and the chamber depth h. Some quantitative data are available for *Tetrahymena pyriformis* (Winet & Jahn 1972, Levandowsky et al 1975, Childress et al 1975) and for various algae: *Euglena viridis* (Wager 1911), *Chlamydomonas nivalis*, and *Dunaliella tertiolecta* (Kessler 1985b, 1986a). The observations on *T. pyriformis* indicate that no patterns form if h is less than a critical value h_c which decreases as N_0 increases. For a given h there is also, therefore, a critical value of N_0. The value of h_c was around 4 mm when N_0 was around 10^6 cells cm^{-3}, but was less than 1 mm when N_0 was as high as 5×10^6 cells cm^{-3}. For the lower cell concentration, the steady-state pattern was in the form of regular dots for slightly supercritical depths, but became more irregular and then gave way to lines as h was increased. The spacing of the dots or lines, λ say, decreased as h was increased (Wille & Ehret 1968); this is opposite to what happens in thermal convection. For the higher concentration the labyrinthine pattern was always seen, even at very small depths.

The existence of a critical cell concentration and a critical depth, the change from dots to filaments as h increases, and the decrease in λ as h increases are also found in suspensions of algae, but λ decreases with time during pattern development. The mechanism of bioconvection is in some respect different for the algae. One dramatic difference in their behavior is

that they are strongly influenced by light; in some species, for example, patterns do not form when the suspension is strongly illuminated (Wager 1911), and shining light from different directions can be used to modify preexisting patterns (Wager 1911, Kessler 1986a, 1989). However, the general observations above refer to patterns that form in the dark or in a dim, nondirected light; so phototaxis is not the explanation for any differences. The other big difference between the algae and *Tetrahymena* is that the former are bottom-heavy and hence gyrotactic. The consequences of this will be discussed below.

In a deep chamber ($\gtrsim 2$ cm) patterns can be observed from the side, and essentially two types of structure are observed. One consists of plumes or streamers plunging from a concentrated layer at the upper surface, which can happen in suspensions of protozoa, bacteria, or algae (Wager 1911, Plesset & Winet 1974, Kessler 1986a); these plumes may exhibit blips (see Section 3.5) at the front or along their length. The other structure has been reported only in algal suspensions, and consists of streamers spontaneously generated in the interior of the suspension, leading ultimately to "bottom-standing plumes"—regularly spaced plumes which occupy only the lowest 2 or 3 cm of the chamber (Wager 1911, Kessler 1985b, 1986a).

In the case of bacteria, the labyrinthine patterns have been seen in shallow layers with a free upper surface (Figure 2*c*). The pattern geometry, however, is a strong function of layer depth. Viewed from the side, a deep chamber reveals no motion at all towards the bottom, but rather complex motions in a well defined region at the top (Figure 2*e*). These will be discussed more fully below.

4.2 *Mechanisms*

Common to all the microorganisms that exhibit bioconvection are (*a*) a greater density than water and (*b*) upswimming. In a fluid of finite depth, upswimming means that cells accumulate near the top surface, so the upper regions of the suspensions are denser than the lower. If the density gradient is high enough the fluid becomes unstable; this leads to an overturning convection, analogous to Rayleigh-Bénard convection in a layer of fluid heated from below.

For organisms that exhibit gyrotaxis (algae) there is a second, independent instability mechanism that leads to spontaneous pattern formation in a uniform, unbounded suspension. Suppose that a small fluctuation causes the cell concentration in a particular blob of fluid to be greater than in its surroundings. This blob, being denser than the surroundings, will sink, thereby generating a velocity distribution with horizontal vorticity, which will focus other cells into the wake of the sinking blob, and a falling concentrated plume will be formed. Gyrotaxis will also,

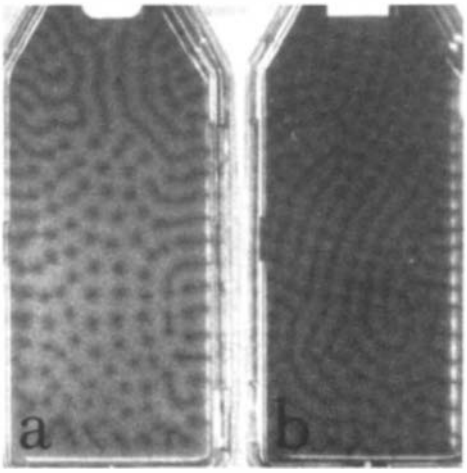

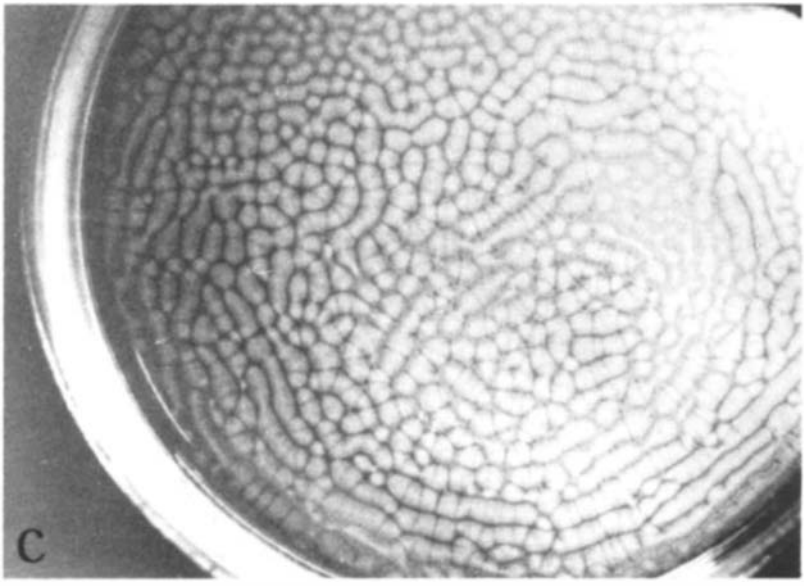

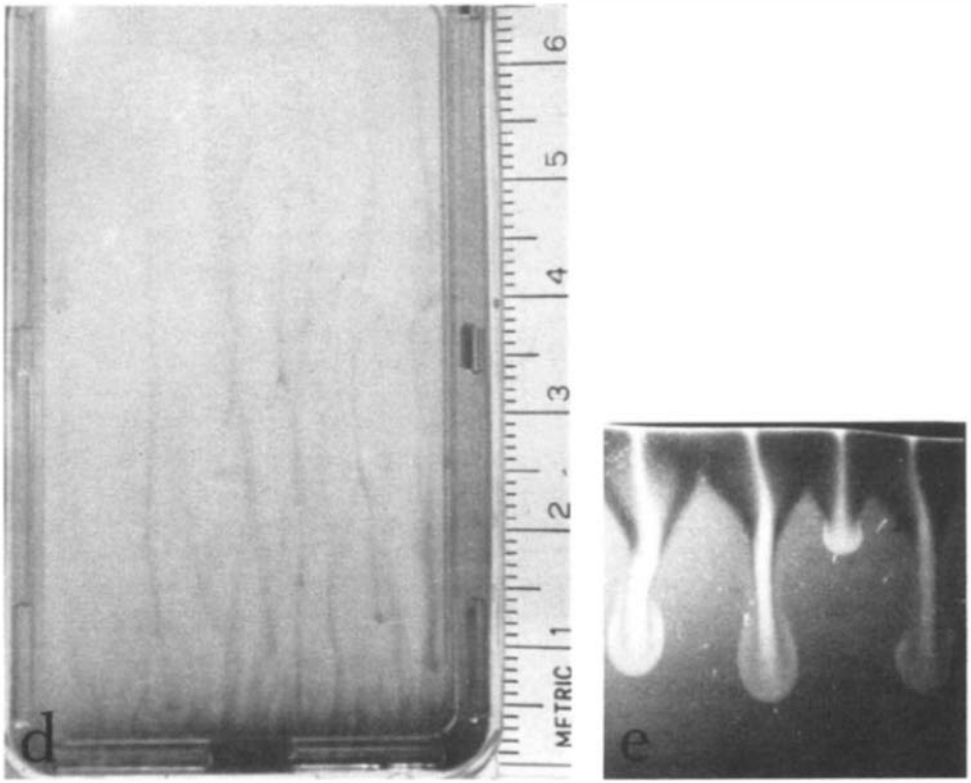

Figure 2 Photographs of bioconvection. (*a*) Steady-state bioconvection in a shallow ($h = 3.2$ mm) suspension of algal cells *Dunaliella tertiolecta* viewed from above: mean concentration $N_0 = 2 \times 10^6$ cells cm^{-3}; breadth of container $d_0 = 4$ cm. (*b*) Transient bioconvection in a slightly deeper ($h = 6.8$ mm) suspension of *D. tertiolecta* viewed from above: $N_0 = 2 \times 10^6$ cells cm^{-3}, $d_0 = 4$ cm. (*c*) Steady-state bioconvection in a suspension of bacteria (*Bacillus subtilis*) viewed in dark field illumination from above: $N_0 = 10^9$ cells cm^{-3}, $h = 2.5$ mm, $d_0 = 8$ cm. This type of pattern was termed "Labyrinthine" by Levandowsky et al (1975). (*d*) Steady-state bioconvection in a deep ($h = 15$ mm) suspension of *C. nivalis* viewed from the side: $N_0 = 10^6$ cells cm^{-3}. Note the occurrence of "bottom-standing plumes," which have transported most of the cells towards the bottom, causing wider spacing at greater heights. (*e*) Bioconvection in a deep and narrow ($h = 1$ mm) suspension of *B. subtilis* viewed in dark field from the side; $N_0 = 10^9$ cells cm^{-3}.

of course, affect the bioconvection patterns generated by the upswimming mechanism in a fluid of finite depth.

Which mechanism leads to the first instability in any particular suspension of gyrotactic cells depends on the relative magnitudes of various time-scales. If the suspension is initially well-stirred—and therefore uniform in concentration—the stirring motions will decay in a time t_d. Supposing this to be short enough, upswimming will tend to set up an unstable density stratification near the top surface in a time t_s and the growth of the overturning instability will take a further time t_{m1}. Meanwhile the essentially uniform suspension well below the surface will become gyrotactically unstable in a time t_{m2}. This instability will be observed first if $t_d < t_{m2} < t_s + t_{m1}$, while the overturning instability will be seen first if $t_d < t_s < t_{m2}$. Hill et al (1989) estimated that the overturning instability will occur first if the fluid layer is sufficiently shallow, but that both mechanisms are represented in Kessler's (1985b, 1986a) experiments. If t_d is longer than the other times, the decaying stirring motions themselves trigger the formation of focussed plumes without requiring the growth of instability from rest.

Direct thermal convection can of course occur in microorganism suspensions if the containing chamber is heated from below or from the sides, or if sufficient heat is absorbed from the illumination. However, bioconvection continues in a layer that is strongly cooled from below, so cannot be a thermal effect (Platt 1961).

The upswimming in aerobic bacterial suspensions (Figure 2*c*,*e*) is a consequence of the tendency to swim (on average), not up a gravitational gradient, but up an O_2 gradient (chemotaxis). There are two important differences. One is that the bacteria consume O_2 and stop swimming when the O_2 concentration, C, becomes too low; this explains the inactivity of individual cells below a certain depth seen in Figure 2*e*. The other is that O_2 can diffuse and, in the presence of fluid motion, is advected. Thus (*a*) the cell swimming velocity $\mathbf{V}_c$ and the cell swimming diffusivity $\mathbf{D}$ which appear in the cell conservation equation (3.7) are functions of C, and (*b*) C itself satisfies a reaction-diffusion equation of the form

$$\frac{\partial C}{\partial t} = -\nabla\cdot(\mathbf{u}C - D_{O_2}\nabla C) - K(C)n. \tag{4.1}$$

where D_{O_2} is the O_2 diffusivity, and the last term represents O_2 consumption by the cells. An interesting feature of the resulting convection is the fact that it is double-diffusive, since D_{O2} and a typical component of $\mathbf{D}$ will have different values. This problem is currently being investigated theoretically. A further complication can arise at high cell concentration, where

one may expect stirring of the medium by the swimming cells. In that case D_{O_2} would depend on the cell concentration.

The mechanism for the band formation in magnetotactic bacteria swimming in a narrow tube cannot be attributed to convective motions driven by gravity. Spormann (1987) was also able to rule out direct magnetic dipole-dipole interactions between cells. Guell et al (1988) have proposed a plausible—but as yet untested—mechanism for band formation, based on the hydrodynamic interaction between neighboring cells. The magnetic field has no direct effect but is important for the purposes of (*a*) causing the cells to concentrate and (*b*) aligning them all in the same direction.

4.3 *Linear Theories*

We begin by considering suspensions of dense cells that do not exhibit gyrotaxis but (on average) swim upwards at all times. We suppose there is a free upper surface at $z = 0$. Plesset & Winet (1974) proposed a two-layer model of the unstable density distribution, with a uniform layer of dense fluid of given depth H overlying a uniform deeper layer of lower density. There was no diffusion—i.e. cell swimming—between the two layers. This basic state breaks down through a Rayleigh-Taylor instability, analyzed fully for viscous fluids by Plesset & Whipple (1974). The theory allowed a prediction of the wavelength of the most unstable disturbance, which agreed quite well with observations on finite depth suspensions of the upswimming ciliate *Tetrahymena pyriformis*, although of course it depends on a visual estimate of H.

The main weakness of this model, like that of using Smith's theory for the blip instability (Section 3.5), is the neglect of cell diffusion, with the result that the proposed basic state is not a solution of the governing equations, in particular the cell conservation equation (3.7). If the cell concentration n_0 is a function of z alone, in a fluid at rest (on average), it will be determined by a balance between upswimming and diffusion to give

$$n_0(z) = N \exp(zV_c/D_v), \tag{4.2}$$

where V_c is the average vertical cell swimming speed and $D_v = D_{zz}$ is the vertical cell diffusivity [both of these can be calculated from the orientation p.d.f. in (3.15)]. N is a normalization constant proportional to the global average cell concentration N_0.

Childress et al (1975) analyzed the linear stability of this basic state in the manner that is standard for convection problems, postulating that

$$\left.\begin{aligned} n &= n_0(z) + \varepsilon n'(z) \exp[i(k_1 x + k_2 y) + \sigma t], \\ \mathbf{u} &= \varepsilon \mathbf{u}'(z) \exp[i(k_1 x + k_2 y) + \sigma t], \end{aligned}\right\} \tag{4.3}$$

etc, where ε is a small amplitude parameter, and using the linearized version of (3.7) and of the Navier-Stokes equations under the Boussinesq approximation:

$$\nabla \cdot \mathbf{u} = 0 \tag{4.4a}$$

$$\rho \frac{D\mathbf{u}}{Dt} = -\nabla p_c - nv\Delta\rho g\mathbf{k} + \nabla \cdot \boldsymbol{\Sigma}. \tag{4.4b}$$

Here p_c is the pressure excess above hydrostatic and $\boldsymbol{\Sigma}$ is the bulk deviatoric stress tensor, taken equal to its Newtonian value $2\mu\mathbf{E}$ since the suspension is supposed dilute. In (3.7) the average cell swimming velocity was taken to be vertically upwards at all times, equal to $V_c\mathbf{k}$, while $\mathbf{D}$ was orthotropic with a horizontal diffusivity D_H different from D_V (Childress et al guessed $D_H/D_V < 1$, whereas the Fokker-Planck theory makes it clear that $D_H/D_V > 1$). The eigenvalue problem boils down to a sixth-order system of ordinary differential equations for the vertical velocity and the concentration perturbation, with suitable boundary conditions at top and bottom.

The theory of Childress et al (1975) was the first self-consistent hydrodynamic theory of the onset of bioconvection. They used it to predict the critical value of the bioconvection Rayleigh number, based on the scale-height D_V/V_c of the density distribution (4.2):

$$\hat{R} = gNv(\Delta\rho/\rho)D_V^2/vV_c^3, \tag{4.5}$$

the critical wavenumber k_c (scaled with V_c/D_V), the growth rate $\sigma D_V/V_c^2$, and the wavenumber k_m at which σ is maximum, all for various values of the dimensionless chamber depth $d = hV_c/D_V$ [we follow the notation of Hill et al (1989)]. The Rayleigh number based on chamber depth is $d^3\hat{R}$. Childress et al found (*a*) that $\hat{R}_c$ decreases as d increases (for a rigid lower boundary and a free upper boundary, for $D_H = D_V$, and for large Schmidt number v/D_V: $\hat{R}_c \approx 470$ when $d = 1$, $\hat{R}_c \sim 4/d$ as $d \to \infty$); (*b*) that $k_c = 0$, i.e. infinite wavelength or pattern spacing, for all values of d; but (*c*) that k_m is finite for $\hat{R} > \hat{R}_c$, increasing rapidly from zero as $\hat{R} - \hat{R}_c$ increases to about $\hat{R}_c$, then leveling off. Thus, given N_0 and hence N, there is indeed a critical depth h_c above which bioconvection will begin (and a critical N_0 for a given h) and the pattern wavelength λ is predicted to fall as h increases above h_c. This agrees well (qualitatively) with experiments on both *Tetrahymena* and on algae, though there are no reports of extremely large wavelengths for depths slightly above critical as the linear theory would suggest.

Quantitatively, Childress et al compared their prediction of k_m with the observed wavelength in two *Tetrahymena* experiments, necessarily making

very rough estimates of some of the parameters. For example, they calculated D_V from Plesset & Winet's (1974) visual estimates of the depth D_V/V_c of the upper, cell-rich layer (around 1 mm), which appeared to be smaller for large cell concentrations, coupled with an independent estimate for V_c (≈ 0.45 mm s^{-1}, so $D_V \approx 4.5 \times 10^{-3}$ cm^2 s^{-1}). Agreement with observation was reasonable (within a factor of 1.5), though it was best if D_H/D_V was taken to be small (≈ 0.1) and not greater than 1 as suggested by the Fokker-Planck theory.

Hill et al (1989) repeated the Childress et al theory for a shallow suspension of algae that exhibit gyrotaxis. The theory was still not "rational" because the cell orientation was taken to be deterministic [given by $\dot{\mathbf{p}} = 0$ in (2.4)], so that $\mathbf{V}_c = V_s\mathbf{P}$ in (3.7), while randomness was allowed for by including cell diffusion (in the absence of data these authors took $D_H = D_V$). The main differences in the results, all directly attributable to gyrotaxis, were as follows. (*a*) The critical wavenumber is finite, not zero, so the absence of very large wavelengths in the observations is no longer a difficulty. (*b*) When the upper surface is rigid, there exist oscillatory modes of instability, and for some parameter values the critical and most unstable disturbances are oscillatory. This is quite different from the case of pure upswimming where the growth rate of unstable disturbances was proved to be real. The physical mechanism for the oscillatory modes comes from gyrotaxis of nonspherical cells in the shear flow at the upper boundary, which causes the horizontal component of the cell's swimming velocity to be opposite to that of the convective flow. Oscillatory patterns have not (yet) been observed.

A complete survey of parameter space was not attempted because, in addition to $\hat{R}$, d, and the Schmidt number, there are two more dimensionless parameters in the problem, the cell eccentricity α_0 and the "gyrotaxis number," $\hat{G} = BV_c^2/D_V$, which is the ratio of the distance a cell will swim in one reorientation time to the depth of the cell-rich layer. There is no change in the prediction that, for fixed $\hat{G}$ and α_0, $\hat{R}_c$ at first decreases as d is increased, then levels off to a constant value as d approaches ∞. The pattern wavelength decreases slightly as d is increased. As $\hat{G}$ or α_0 is increased, however, $\hat{R}_c$ rises while the pattern wavelength falls; the latter variation is quite marked, so a good comparison with experiment requires accurate estimation of these parameters.

Hill et al tested the theory quantitatively against the experiments of Kessler (1985b, 1986a) on *Chlamydomonas nivalis*, using independent measurements or estimates of quantities such as B, V_C, and D_V. Both the swimming speed and the diffusivity are considerably smaller than for *Tetrahymena*; Hill et al took $B = 3.4$ s, $V_c = 100$ μm s^{-1}, and $D_V \approx 5 \times 10^{-4}$ cm^2 s^{-1} (so $D_V/V_c \approx 0.5$ mm and $\hat{G} \approx 0.7$), while the later

observations of Häder & Hill (1991) (see Pedley & Kessler 1990) suggest $V_c = 32\ \mu\text{m s}^{-1}$ and $D_V \approx 6.7 \times 10^{-6}\ \text{cm}^2\ \text{s}^{-1}$ (giving $D_V/V_c \approx 0.02$ mm, $\hat{G} \approx 5.2$). Hill et al's parameter values gave a predicted wavelength of 2–3 cm, much larger than for the observed, steady-state, nonlinear convection patterns in a chamber 1 cm deep, but in good agreement with the first rather irregular patterns to form in a recently stirred suspension. However, the larger estimate of $\hat{G}$ based on Häder & Hill's data must call these comparisons into question. We still need quantitative experiments in which all relevant parameters are measured as carefully as possible. It should be mentioned that swimming algae may inhibit accurate measurements by accumulating at bounding surfaces of the fluid. They may adhere to the walls and even convert the free surface at the top to a virtually rigid surface, by interacting and sticking to one another. These accumulations can be dislodged by shaking, but they may produce a secular variation in the boundary conditions and cell concentration.

The purely gyrotactic instability of an infinite, uniform suspension was analyzed by Pedley et al (1988) using the "old" continuum model ($\mathbf{V}_c = V_s\mathbf{P}$, $\mathbf{D}$ is isotropic) and by Pedley & Kessler (1990) using the "new" one based on the Fokker-Planck equation. The uniformity of the basic state makes this stability problem particularly simple, the ordinary differential equations for n' and $\mathbf{u}'$ in (4.3) having only constant coefficients. Both theories, in fact, led to quadratic equations for the growth-rate σ. The main results of the "old" theory (Pedley et al 1988) were as follows. (*a*) If there is no gyrotaxis there is no instability. (*b*) Analytical estimates of the critical and the most unstable wavelengths λ were made, the latter corresponding for *C. nivalis* to 9 mm for a convection pattern made up of rolls, and 13 mm for one made up of squares. These values are well above the plume spacing observed in a deep chamber, about 1–3 mm. The discrepancy was attributed to the nonlinear nature of the fully-developed pattern, since λ is observed to decrease with time after the beginning of an experiment. (*c*) If the cells are sufficiently elongated ($\alpha_0 > \frac{1}{3}$) both the critical and the most unstable disturbances are predicted to be three-dimensional, corresponding to blobs (or blips) rather than the usual plumes. Despite involving a variety of additional effects—such as a non-zero (but divergence-free) intrinsic stresslet distribution in the basic state, from (2.6), and asymmetric contributions to the particle stress tensor as a result of the external couple—the more rational, Fokker-Planck theory did not yield novel predictions. Indeed, the predicted most unstable wavelength for *C. nivalis* remained at 9 mm. The only new results were that three-dimensional disturbances, with a nonzero vertical wavenumber, would always propagate upwards and would always decay. The former could have been predicted from the earlier theory, and the latter contradicts

prediction (*c*) above, revealing it to be an artifact of the nonrational model. Future work *must* use a rational theory and earlier predictions such as the oscillatory instabilities of Hill et al (1989) need reexamination.

4.4 *Nonlinear Models*

There are several approaches to the nonlinear modeling of bioconvection, all commonplace in the analysis of thermal convection. They can be classified under three headings: (*a*) weakly nonlinear theory, (*b*) ad hoc models for steady-state bioconvection, and (*c*) numerical simulation by integration of the Navier-Stokes equation together with either the cell conservation equation or a Monte Carlo simulation of the trajectories of individual cells. These have all been attempted but it is fair to say that none has yet led to a definitive, quantitative description of steady-state bioconvection, nor to good predictions of the pattern shapes or spacing.

WEAKLY NONLINEAR THEORY For standard convection problems the Rayleigh number R is taken to be close to its critical value R_c, so that $R - R_c = \varepsilon^2 R_2 + \mathcal{O}(\varepsilon^3)$ where ε is a small parameter (Newell & Whitehead 1969). The dependent variables are expanded as power series in ε, while the time-scale for growth or decay of the disturbances is $\mathcal{O}(\varepsilon^{-2})$. At $\mathcal{O}(\varepsilon)$ the linear theory is recovered, and the first-order disturbance quantities can be written as linear combinations of modes with horizontal wavenumber k (e.g. $\cos kx$, $\cos ky$) and with time-dependent amplitudes. The solvability condition at $\mathcal{O}(\varepsilon^2)$ determines R_c and the critical wavenumber k_c. The second-order problem has to be solved, and the solvability condition at $\mathcal{O}(\varepsilon^3)$ leads to nonlinear ordinary differential equations (Landau equations) for the amplitudes, which contain R_2 as a parameter. From these it can be determined whether the bifurcation at $R = R_c$ is sub- or supercritical for the different modes, whether the resulting small—but finite—amplitude disturbances (when they exist) are stable or unstable, and hence, for a supercritical bifurcation, what will be the preferred mode (pattern) in practice.

This type of theory could presumably be used to analyze gyrotactic bioconvection, extending the linear theories of Pedley et al (1988, 1990) or of Hill et al (1989), but this has not yet been done. Hitherto, weakly nonlinear theory has been applied only to the case of bioconvection of pure upswimmers, and the standard approach does not work because k_c is zero (Childress et al 1975). In an unpublished manuscript, Childress & Spiegel (1980, personal communication) showed that if ε^{-2} is again taken as the time scale for growth of disturbances, $R - R_c$ has to be $\mathcal{O}(\varepsilon)$, the horizontal length scale is $\mathcal{O}(\varepsilon^{-1/2})$, and the solvability condition at $\mathcal{O}(\varepsilon^3)$ yields a *partial* differential equation with a nontrivial solution for the

amplitude as a function of time and horizontal coordinate. They found steady-state solutions of this equation and deduced that the bifurcation is subcritical, with the consequence that the observed pattern cannot be predicted. The reader is referred to Chapman & Proctor (1980) for a published version of this method.

AD HOC MODELS In the same unpublished manuscript, Childress & Spiegel looked for a steady-state model in which an isolated blob of high cell concentration could persist as a solution of the governing equations. They neglected both fluid inertia and cell diffusion, and examined only two-dimensional flow in a vertical plane. They proposed that the blob, being a source of downward momentum, would generate a recirculating flow in a fluid of finite depth with laterally periodic boundary conditions; adding a constant upswimming velocity to this velocity field inside the blob could be consistent with a fixed region of closed cell trajectories (Figure 3). Because the boundary C of the blob is unknown a priori, it is difficult to construct a mathematical solution for such a flow, but Childress & Spiegel developed a variational approach and were able to make it plausible that such blobs could exist. An estimate of blob spacing could be made by maximizing the area (corresponding, in three dimensions, to the volume) of the blob, though it was not clear why such a maximization principle should be imposed. Although this was a very interesting model, it may not have much relevance to bioconvection patterns that extend from the top to the bottom of a fluid layer, or consist of long streamers or plumes. A modified version of the model may, indeed, have more relevance to the analysis of "bubbles" in fluidized beds.

Pedley (1988) tried to construct a somewhat similar model of "bottom-standing plumes" in suspensions of gyrotactic algae, again considering a horizontally periodic pattern in two dimensions (Figure 4). The negative buoyancy of a concentrated central plume drives a downflow, compensated for by a neighboring upflow driven by an induced pressure gradient. Cells are advected with the flow, but also swim relative to it; gyrotaxis causes them to swim across the flow streamlines and to be focussed laterally into the plume again. Given a plume spacing ℓ, a scale for the height H of the plumes can be determined by equating the time for advection to that height, W_0/H (where W_0 is a typical vertical fluid velocity), to the time for swimming laterally a distance ℓ, $V_s B\omega/\ell$ (from 3.2c) which is proportional to $V_s B W_0/\ell^2$. Hence $\ell/H = BV_s/\ell = \varepsilon_1$, say, and the model is self-consistent if ε_1 is small. For *C. nivalis*, $BV_s \approx 0.3$ mm and ℓ is observed to be ≈ 3 mm, so $\varepsilon_1 \approx 0.1$ and $H \approx 30$ mm, consistent with casual observation. If one assumes that, in the plume, the dominant terms in the cell balance equation are horizontal swimming and diffusion, as in (3.10), the plume

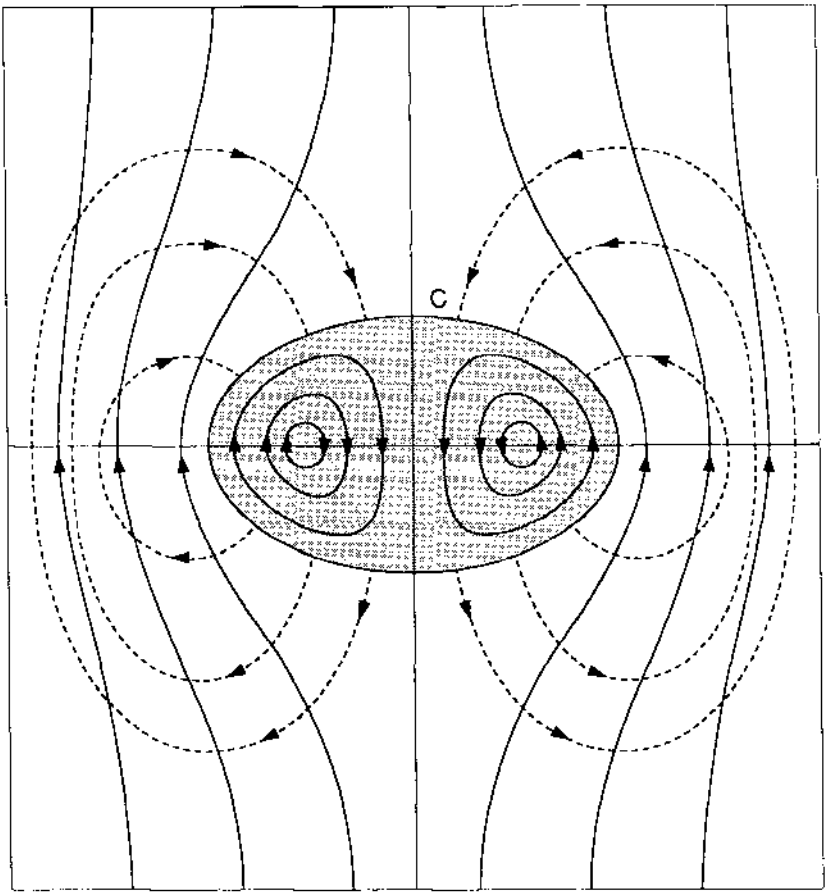

Figure 3 Two-dimensional model for a concentrated blob of cells, driving a fluid motion because of the cells' excess density but remaining stationary because of their upswimming. Solid curves are cell trajectories; broken curves are flow streamlines. (Copied from Childress & Spiegel 1980, with permission.)

width δ is found to be $D\ell/W_0BV_c$. The concentration distribution is proportional to $\mathrm{sech}^2(x/\delta)$, as found by Kessler (1985b), but the proportionality factor will be a function of z (see Figure 4 for the coordinate system). Further, if inertia is negligible in the vertical momentum equation, then the latter becomes a balance between buoyancy and viscosity, so that

$$W_0 \sim \ell^2 v \Delta\rho g N_0/\mu. \tag{4.6}$$

Thus the scales for all important quantities are determined, given ℓ.

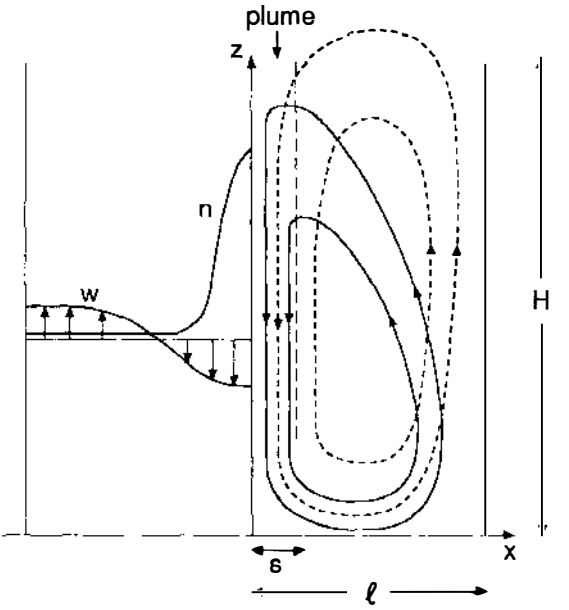

Figure 4 Two-dimensional model for bottom-standing plumes. Solid curves are cell trajectories; broken curves are flow streamlines. Note the lateral component of cell swimming as a result of gyrotaxis. Conjectured profiles of cell concentration n and vertical fluid velocity w are indicated.

An additional equation linking the various parameters can be derived from an overall energy balance. The whole motion is driven by the microorganisms swimming upwards. Hence, in a steady state, the total rate of increase of potential energy, $N_0 v \Delta\rho g V_s$ per unit volume, must balance the overall rate of viscous dissipation, $\mu(W_0/\ell)^2$ per unit volume, or

$$W_0^2 \sim \ell^2 v \Delta\rho g N_0 V_s/\mu. \tag{4.7}$$

Combining (4.6) and (4.7) does indeed give an estimate for ℓ, albeit somewhat small (<1 mm when $N_0 \sim 10^6$ cells cm^{-3}), but these equations also predict $W_0 \sim V_s$, whereas it is observed that convection speeds are significantly larger than cell swimming speeds. The error probably lies in some of the assumptions that went into (4.6), such as the neglect of fluid inertia.

A different estimate of an upper bound for plume spacing arises from Kessler's (1986b) observation that there is a maximum radius R_1 to the region from which an axisymmetric plume can be generated from a background concentration N_0, since for larger radii a singularity appears in the

concentration distribution [see the discussion following (3.20) above]. In obtaining that result, Kessler assumed no z-dependence and no pressure gradient, whereas both are present in bottom-standing plumes, so the estimate is more of conceptual interest than of quantitative value (though the estimate of R_1 is again around 1 mm for $N_0 = 10^6$ cells cm^{-3}, not much less than the observed half-spacing).

NUMERICAL SIMULATION Full numerical integrations of the governing equations in convection studies are costly in computer time and require as deep an interpretation as experimental observations. Very few have been devoted to bioconvection. Harashima et al (1988) solved the incompressible Navier-Stokes and cell conservation equations [(4.4) and (3.7)] in two dimensions. They followed Childress et al (1975) in considering pure upswimmers, such as *T. pyriformis*, so $\mathbf{V}_c = V_s\mathbf{k}$, with isotropic cell diffusivity (except for one run in which D_H/D_V was taken to be 10). Their computational domain was a wide, shallow box with aspect ratio 8 and shear-free upper surface; the ratio d of box depth to the scale-height D_V/V_s of the equilibrium concentration distribution (4.2) was given a range of values from 2 to 80. The initial condition was taken to be one of uniform concentration N_0, which was varied from run to run, together with an infinitesimal random vorticity distribution. The first thing to happen, therefore, was that the cells swam up, and the concentration distribution evolved towards (4.2). In all the runs described the Rayleigh number $\hat{R}$ (Equation 4.5) was above its critical value, so after a certain time disturbances began to develop in the uppermost unstable zone. The growth rate and wavenumber of these disturbances agreed extremely well with those predicted for the most unstable disturbance by Childress et al (1975). These disturbances led to falling streamers [cf Figure 1 of Harashima et al (1988) and Figure 1 of Plesset & Winet (1974)].

As time went on, however, the pattern changed via a number of isolated events, at which the number of vertical columns decreased by one, separated by periods of gradual evolution. Eventually steady-state convection rolls were set up, filling the whole depth of the box. In one example shown there were three rolls in the box, whereas the initial disturbance had eight falling streamers. In another example, the final number of rolls (three or four) depended on the initial condition. The steady-state convection pattern was clearly related to the depth of the fluid layer, as for thermal convection, while the initial disturbance was related to the characteristics of the equilibrium density distribution. Harashima et al (1988) proposed *minimum total potential energy* as a principle for the determination of the steady-state roll size (pattern spacing) for a given value of $\hat{R}$ and for a given size box. Their results were reasonably consistent with that principle.

An earlier two-dimensional simulation was provided by Childress & Peyret (1976), who also integrated the Navier-Stokes equations (4.4) but instead of using the continuum cell conservation equation (3.7) they treated the cells as individual moving points each of which exerts a force on the fluid and moves relative to the fluid by a superposition of pure upswimming and a random walk. From an initial condition in which all the cells (756 of them) were in a compact region in the middle of the computational box (aspect ratio 2), states could develop in which, depending on the parameters, (*a*) the cells remained in a single compact region, driving a recirculating flow (cf their Figure 4.2), or (*b*) they could form two compact regions (convection rolls), or (*c*) they could become fairly dispersed, but still driving a bulk flow. It was not clear, however, whether a statistically steady-state convection pattern had been achieved in these examples when the computation was stopped.

There are as yet no published simulations of gyrotactic bioconvection, although the early stages of pattern formation can be seen in some preliminary computations by J. M. Rees (personal communication) using the old continuum model of Pedley et al (1988).

5. EXPLOITATION

Microorganisms interact with their physical environment as individual automata. Gravity, shear, illumination, and other influences cause them to swim, on average, in particular directions. Eventually this directed swimming results in local accumulations of organisms. A sufficient concentration of them in some region of fluid results in density changes that drive collective dynamical patterns. Both the individual and the collective dynamics can provide benefits to the organisms, e.g. improve their growth or chances of survival. Some of the locomotory phenomena can also be exploited for biotechnology and research.

INDIVIDUAL DYNAMICS Automatic upward locomotion of photosynthetic cells keeps them near the surface where the light can penetrate; there is thus a strong evolutionary pressure for algal cell types that swim upward to be selected. Other organisms, such as *Bacillus subtilis* as demonstrated above, prefer particular ranges of oxygen concentration. Yet others prefer no oxygen at all, for example the magnetotactic bacteria that contain magnetic particles. These "magnetosomes" guide the cells along the Earth's magnetic field lines toward bottom sediments (Guell et al 1988).

Bioconvection due to the concentrated cell populations that result from upswimming can be avoided when the convective modes are damped by a

porous medium that is sufficiently open to allow passage of the organisms through the interstitial spaces yet sufficiently tight that the downflow driven by the resulting density difference is slower than the cell swimming speed. Snow, sand, and cotton wool are examples of such media. The populations of algae that accumulate over cotton wool or cloth can be harvested (Kessler 1982, 1984a, 1986a); the method can also be used to separate rapidly swimming cells from slower ones. In a natural setting, the same process generates snow banks colored green or reddish by algae that have swum up from the soil through the meltwater (Hoham 1980); *Chlamydomonas nivalis* is one such snow alga. A spectacular antarctic version of the phenomenon (Everson 1987) surely affects albedo and therefore the entire water-related ecology.

Self-harvesting of flagellates over porous media also occurs in stagnant ponds which are partly covered by floating mats of filamentary blue green algae. It is unclear whether there is a direct benefit, but the very marked increase in the number of swimmers on the mats, compared with regions of open water, suggests that the self-concentration may enhance the frequency of interaction among the organisms and thus have biological significance, for example in the mating of motile gametes or in the predator-prey balance of various upswimming species.

The existence of gyrotactic focusing can be used to rule out certain proposed mechanisms for geotaxis of swimming cells. Cells suspended in a one-meter tall cylindrical Poiseuille flow swim toward the axis when the flow is vertically downward and toward the periphery when it is upward. These observations show that geotaxis does not depend on the pressure or pressure gradient, as has been proposed (Levandowsky & Kaneta 1987). Closing the water circuit in an algal focusing experiment demonstrates that dissolved gas concentration gradients play no role in the cells' upswimming. Focusing in the dark eliminates upswimming responses that depend on light.

Gyrotactic focusing can also be used to separate microorganisms having different locomotory characteristics. For example, fast swimmers can be separated from slow ones, cells where random swimming dominates can be separated from more deterministically oriented ones, and cells whose trajectories are strongly oriented by phototaxis can be separated from light insensitive ones. The feasibility of gyrotaxis as a hydrodynamic cell separation technique has been demonstrated (G. J. Morris & J. O. Kessler, unpublished).

There have been no reports of gyrotactic focusing in nature, probably because no one has looked for evidence of it. Langmuir circulations (Leibovich 1983) are one type of flow where large-scale concentrations of

cells might be expected, focused into vertical sheets beneath the windrows. Another possible scenario for natural focusing is provided by the mechanism for predation discussed in Section 3.1. It is conceivable that such purely physical mechanisms for bringing individuals close to each other could have had considerable biological importance in the early development of marine life.

COLLECTIVE DYNAMICS There are many possibilities for the natural exploitation of bioconvection. Bioconvection is associated with regularly spaced regions of high and low cell concentration, correlated with patterns of downward and upward streaming, which is much more rapid than an individual organism's swimming (or sedimentation) relative to still water. Such bio-advection may be involved in the vertical migrations of algal blooms. Bioconvective streaming can also enhance mixing, as in the case where oxygen is rapidly supplied to an entire population of aerobic bacteria (Figure 2*e*). This is a form of active transport which augments diffusion. Spatial variations in organism concentration create environments of mottled illumination; this self-shading pattern, developed by the population as a whole, enables individual cells to swim into a region of preferred light intensity and may have implications for population dynamics (Noever 1990b).

If these effects occur naturally, one would expect them to be in quiet pools or puddles. Agitation of large bodies of water would tend to destroy bioconvection, and turbulent advection would greatly exceed the transport of cells by swimming. Furthermore, even in still water, poor contrast would usually inhibit observation of collective behavior. Some cases of bioconvection and self-gyrotactic focusing have been anecdotally reported. One of us (JOK) has found dense algal cell blooms that exhibit bioconvection in small natural puddles. It is likely that bacterial convection in thin fluid layers will eventually be found quite routinely.

Finally, it is worth noting that swimming cells can provide a unique service to the fluid mechanical study of convection, because the cells constitute both the driving force for the convection and the marker particles that allow the flow to be visualized. As the flow changes, after a change in external conditions, the cells reorganize themselves to make the new downflow regions as clearly visible as the old ones. We have seen this most clearly in some unpublished studies of bioconvection in a container on a rotating table (Department of Applied Mathematics and Theoretical Physics, Cambridge University, 1987) where all the phenomena reported for thermal convection in a rotating chamber [convective rings, vortex grid, irregular vortex pattern (Boubnov & Golitsyn 1986)] could be observed more simply.

ACKNOWLEDGMENTS

We should like to acknowledge with thanks the support of the SERC, the National Science Foundation, through grant No. INT-8922466, and Ralph and Alice Sheets who supported this work through the University of Arizona Foundation.

Literature Cited

Armitage, J. P., Macnab, R. M. 1987. Unidirectional intermittent rotation of the flagellum of *Rhodobacter Sphaeroides*. *J. Bacteriol.* 169: 517–18

Batchelor, G. K. 1970. The stress system in a suspension of force-free particles. *J. Fluid Mech.* 41: 545–70

Berg, H. C. 1983. *Random Walks in Biology*. Princeton: Princeton Univ. Press

Berg, H. C., Brown, D. A. 1972. Chemotaxis in *Escherichia coli* analysed by three-dimensional tracking. *Nature* 239: 500–4

Bishop, D. W. 1962. Sperm motility. *Physiol. Rev.* 42: 1–59

Bold, H. C., Wynne, M. J. 1978. *Introduction to the Algae: Structure and Reproduction*. Englewood Cliffs: Prentice-Hall

Boubnov, B. M., Golitsyn, G. S. 1986. Experimental study of convective structures in rotating fluids. *J. Fluid Mech.* 167: 503–31

Brennen, C., Winet, H. 1977. Fluid mechanics of propulsion by cilia and flagella. *Annu. Rev. Fluid Mech.* 9: 339–98

Brenner, H. 1974. Rheology of a dilute suspension of axisymmetric Brownian particles. *Int. J. Multiphase Flow* 1: 195–341

Brenner, H., Weissman, M. H. 1972. Rheology of a dilute suspension of dipolar spherical particles in an external field. II. Effect of rotary Brownian motion. *J. Colloid Interface Sci.* 41: 499–531

Bretherton, F. P., Rothschild, Lord 1961. Rheotaxis of spermatozoa. *Proc. R. Soc. London Ser. B* 153: 490–502

Brinkmann, K. 1968. An Phasengrenzen induzierte ein und zweidimensionale Kristallmuster in Kulturen von *Euglena gracilis*. *Z. Pflanzen Physiol.* 59: 364–76

Chapman, C. J., Proctor, M. R. E. 1980. Nonlinear Rayleigh Bénard convection between poorly conducting boundaries. *J. Fluid Mech.* 101: 759–82

Charlson, R. J., Lovelock, J. E., Andreae, M. O., Warren, S. G. 1987. Oceanic phytoplankton, atmospheric sulphur, cloud albedo and climate. *Nature* 326: 655–61

Childress, S. 1981. *Mechanics of Swimming and Flying*. Cambridge: Cambridge Univ. Press

Childress, S., Levandowsky, M., Spiegel, E. A. 1975. Pattern formation in a suspension of swimming micro-organisms. *J. Fluid Mech.* 69: 595–613

Childress, S., Percus, J. K. 1981. Nonlinear aspects of chemotaxis. *Math. Biosciences* 56: 217–37

Childress, S., Peyret, R. 1976. A numerical study of two-dimensional convection by motile particles. *J. Mécanique* 15: 753–79

Colombetti, G., Lenci, F. 1983. Photoreception and photomovement in microorganisms. In *The Biology of Photoreception*, ed. D. J. Cosens, D. Vince-Prue, pp. 399–422. Cambridge: Cambridge Univ. Press

Ettl, H. 1976. Die Gattung *Chlamydomonas* Ehrenberg. *Beih. Nova Hedwigia* 49: 1–1122

Everson, I. 1987. Life in a cold environment. In *Antarctic Science*, ed. D. W. H. Walton, pp. 71–125. Cambridge: Cambridge Univ. Press

Fenchel, T., Finlay, B. J. 1984. Geotaxis in the ciliated protozoon *Loxodes*. *J. Exp. Biol.* 110: 17–33

Fenchel, T., Finlay, B. J. 1986. Photobehaviour of the ciliated protozoon *Loxodes*: taxic, transient, and kinetic responses in the presence and absence of oxygen. *J. Protozool.* 33: 139–45

Finlay, B. J., Berninger, U.-G., Stewart, L. J., Hindle, R. M., Davison, W. 1987. Some factors controlling the distribution of two pond-dwelling ciliates with algal symbionts (*Frontonia vernalis* and *Euplotes daidaleos*). *J. Protozool.* 34: 349–56

Floyd, G. L., O'Kelley, C. J. 1989. Phylum Chlorophyta Class Ulvophyceae. In *Handbook of Protoctista*, ed. L. Margulis, J. O. Corliss, M. Melkonian, D. J. Chapman, pp. 617–35. Boston: Jones and Bartlett

Foster, K. W., Smyth, R. D. 1980. Light antennas in phototactic algae. *Microbiol. Rev.* 44: 572–630

Fraenkel, G. S., Gunn, D. L. 1940. *The Orientation of Animals*. Oxford: Clarendon

Guell, D. C., Brenner, H., Frankel, R. B., Hartman, H. 1988. Hydrodynamic forces and band formation in swimming magnetotactic bacteria. *J. Theor. Biol.* 135: 525–42

Häder, D.-P. 1987. Polarotaxis, gravitaxis and vertical phototaxis in the green flagellate *Euglena gracilis*. *Arch. Microbiol.* 147: 179–83

Häder, D.-P., Hill, N. A. 1991. Tracking and averaging the swimming trajectories of *Chlamydomonas nivalis*. In preparation.

Häder, D.-P., Tevini, M. 1987. *General Photobiology*, Chapter 12. Oxford: Pergamon

Hall, W. F., Buesenberg, S. N. 1969. Viscosity of magnetic suspensions. *J. Chem. Phys.* 51: 137–45

Harashima, A., Watanabe, M., Fujishiro, I. 1988. Evolution of bioconvection patterns in a culture of motile flagellates. *Phys. Fluids* 31: 764–75

Hart, A., Edwards, C. 1987. Buoyant density fluctuations during the cell cycle of *Bacillus subtilis*. *Arch. Microbiol.* 147: 68–72

Haupt, W., Feinleib, M. E. 1979. *Physiology of Movements*. Berlin: Springer

Hemmersbach-Krause, R., Häder, D.-P. 1990. Negative gravitaxis (Geotaxis) of paramecium—demonstrated by image analysis. *Appl. Micrograv. Technol.* 2: 221–23

Hill, N. A., Pedley, T. J., Kessler, J. O. 1989. The growth of bioconvection patterns in a suspension of gyrotactic micro-organisms in a layer of finite depth. *J. Fluid Mech.* 208: 509–43

Hinch, E. J., Leal, L. G. 1972a. The effect of Brownian motion on the rheological properties of a suspension of non-spherical particles. *J. Fluid Mech.* 52: 683–712

Hinch, E. J., Leal, L. G. 1972b. Note on the rheology of a dilute suspension of dipolar spheres with weak Brownian couples. *J. Fluid Mech.* 56: 803–13

Hoham, R. W. 1980. Unicellular chlorophytes-snow algae. In *Phytoflagellates*, ed. E. R. Cox, pp. 61–84. N.Y. & Amsterdam: Elsevier

Jeffery, G. B. 1922. The motion of ellipsoidal particles immersed in a viscous fluid. *Proc. R. Soc. London Ser. A* 102: 161–79

Joseph, D. D., Lundgren, T. S. 1973. Quasi-linear Dirichlet problems driven by positive sources. *Arch. Rational Mech. Anal.* 49: 241

Katz, D. F., Pedrotti, L. 1977. Geotaxis by motile spermatozoa: hydrodynamic reorientation. *J. Theor. Biol.* 67: 723–32

Kawakubo, T., Tsuchiya, Y. 1981. Diffusion coefficient of *Paramecium* as a function of temperature. *J. Protozool.* 28: 342–44

Kessler, J. O. 1982. Algal cell harvesting. *U.S. Patent No. 4,324,067*

Kessler, J. O. 1984a. Algal cell growth, modification and harvesting. *U.S. Patent No. 4,438,591*

Kessler, J. O. 1984b. Gyrotactic buoyant convection and spontaneous pattern formation in algal cell cultures. In *Nonequilibrium Cooperative Phenomena in Physics and Related Fields*, ed. M. G. Velarde, pp. 241–48. New York: Plenum

Kessler, J. O. 1985a. Hydrodynamic focusing of motile algal cells. *Nature* 313: 218–20

Kessler, J. O. 1985b. Co-operative and concentrative phenomena of swimming micro-organisms. *Contemp. Phys.* 26: 147–66

Kessler, J. O. 1986a. The external dynamics of swimming micro-organisms. In *Progress in Phycological Research*, ed. F. E. Round, D. J. Chapman, Vol. 4, pp. 257–307. Bristol: Biopress

Kessler, J. O. 1986b. Individual and collective dynamics of swimming cells. *J. Fluid Mech.* 173: 191–205

Kessler, J. O. 1989. Path and pattern—the mutual dynamics of swimming cells and their environment. *Comments Theor. Biol.* 1: 85–108

Kessler, J. O. 1990. Theory and experimental results on gravitational effects on monocellular algae. *Adv. Space Res.*, Proc. 28th meeting of COSPAR. Oxford: Pergamon

Kessler, J. O., Hill, N. A., Häder, D.-P. 1991. Orientation of swimming flagellates by simultaneously acting external factors. Submitted to *J. Phycol.*

Lapidus, I. R., Welch, M., Eisenbach, M. 1988. Pausing of flagellar rotation is a component of bacterial motility and chemotaxis. *J. Bacteriol.* 170: 3627–32

Leal, L. G., Hinch, E. J. 1971. The effect of weak Brownian rotations on particles in shear flow. *J. Fluid Mech.* 46: 685–703

Leal, L. G., Hinch, E. J. 1972. The rheology of a suspension of nearly spherical particles subject to Brownian rotations. *J. Fluid Mech.* 55: 745–65

Leedale, G. F. 1967. *Euglenoid Flagellates*. Englewood Cliffs: Prentice-Hall

Leibovich, S. 1983. The form and dynamics of Langmuir circulations. *Annu. Rev. Fluid Mech.* 15: 391–427

Levandowsky, M., Childress, W. S., Spiegel, E. A., Hutner, S. H. 1975. A mathematical model of pattern formation by swimming micro-organisms. *J. Protozool.* 22: 296–306

Levandowsky, M., Kaneta, P. J. 1987. Behaviour in Dinoflagellates. In *The Biology of the Dinoflagellates*, ed. F. J. R. Taylor, pp. 360–97. Oxford: Blackwell

Lighthill, J. 1975. *Mathematical Biofluiddynamics*. Philadelphia: SIAM
Lighthill, J. 1976. Flagellar hydrodynamics. *SIAM Rev.* 18: 161–230
Loeffer, J. B., Mefferd, R. B. 1952. Concerning pattern formation by free-swimming micro-organisms. *Am. Nat.* 86: 325–29
Melkonian, M. 1989. Phylum Chlorophyta Class Chlorophyceae. In *Handbook of Protoctista*, ed. L. Margulis, J. O. Corliss, M. Melkonian, D. J. Chapman, pp. 608–18. Boston: Jones and Bartlett
Neidhardt, F. C., Ingraham, J. L., Schaechter, M. 1990. *Physiology of the Bacterial Cell*. Sunderland, MA: Sinauer
Nelson, D. C., Jørgensen, B. B., Revsbech, N. P. 1986. Growth pattern and yield of a chemoautotropic *Beggiatoa* sp. in oxygen-sulfide micro-gradients. *Appl. and Environ. Microbiol.* 52: 225–33
Nettleton, R. M., Mefferd, R. B., Loeffer, J. B. 1953. Pattern formation in concentrated particulate suspensions. *Am. Nat.* 87: 117–18
Newell, A. C., Whitehead, J. A. 1969. Finite bandwidth, finite amplitude convection. *J. Fluid Mech.* 38: 279–303
Noever, D. A. 1990a. Fractal dimension of bioconvection patterns. *J. Phys. Soc. Jpn.* 59: 3419–22
Noever, D. A. 1990b. Bioconvective patterns, synchrony and survival. *Phys. Rev. Lett.* 65: 1953–56
Nultsch, W., Häder, D.-P. 1988. Photomovement in motile microorganisms. *Photochem. Photobiol.* 47: 837–69
Nultsch, W., Hoff, E. 1973. Investigations on pattern formation in Euglenae. *Arch. Protistenk.* 115: 336–52
Pedley, T. J. 1988. Bottom-standing plumes in gyrotactic bioconvection. *Bull. Am. Phys. Soc.* 33: 2282 (Abstr.)
Pedley, T. J., Hill, N. A., Kessler, J. O. 1988. The growth of bioconvection patterns in a uniform suspension of gyrotactic micro-organisms. *J. Fluid Mech.* 195: 223–37
Pedley, T. J., Kessler, J. O. 1987. The orientation of spheroidal micro-organisms swimming in a flow field. *Proc. R. Soc. London Ser. B* 231: 47–70
Pedley, T. J., Kessler, J. O. 1990. A new continuum model for suspensions of gyrotactic micro-organisms. *J. Fluid Mech.* 212: 155–82
Pelczar, M. J., Chan, E. C. S., Krieg, N. R. 1986. *Microbiology*. New York: McGraw-Hill
Pfennig, N. 1962. Beobachtungen über das Schwärmen von *Chromatium okenii*. *Arch. Mikrobiol.* 42: 90–95
Platt, J. R. 1961. "Bioconvection patterns" in cultures of free-swimming organisms. *Science* 133: 1766–67
Plesset, M. S., Whipple, C. G. 1974. Viscous effects in Rayleigh-Taylor instability. *Phys. Fluids* 17: 1–7
Plesset, M. S., Winet, H. 1974. Bioconvection patterns in swimming microorganism cultures as an example of Rayleigh-Taylor instability. *Nature* 248: 441–43
Prescott, L. M., Hurley, J. P., Klein, D. A. 1990. *Microbiology*. Dubuque: W. C. Brown
Roberts, A. M. 1970. Motion of spermatozoa in fluid streams. *Nature* 228: 375–76
Roberts, A. M. 1972. Gravitational separation of X and Y spermatozoa. *Nature* 238: 223–25
Roberts, A. M. 1975. The biassed random walk and the analysis of micro-organism movement. In *Swimming and Flying in Nature*, ed. T. Y.-T. Wu, C. J. Brokaw, C. Brenner, Vol. 1. New York: Plenum
Rothschild, Lord 1949. Measurement of sperm activity before artificial insemination. *Nature* 163: 358–59
Rothschild, Lord 1962. Sperm movement-problems and observations. In *Spermatozoan Motility*, pp. 13–29. Washington, DC: AAAS
Rüffer, U., Nultsch, W. 1985. High-speed cinematographic analysis of the movement of *Chlamydomonas*. *Cell Motility* 5: 251–63
Schnitzer, M. J., Block, S. M., Berg, H. C., Purcell, E. M. 1990. Strategies for Chemotaxis. In *Biology of the Chemotactic Response*, ed. J. P. Armitage, J. M. Lackie, *46th Symp. Soc. Gen. Microbiol*, pp. 15–34. Cambridge: Cambridge Univ. Press
Shioi, J., Dang, C. V., Taylor, B. L. 1987. Oxygen as attractant and repellant in bacterial chemotaxis. *J. Bacteriol.* 169: 3118–23
Sleigh, M. A. 1973. *Cilia and Flagella*. London: Academic
Smith, M. K. 1989. The axisymmetric long-wave instability of a concentric two-phase pipe flow. *Phys. Fluids* A1: 494–506
Spormann, A. M. 1987. Unusual swimming behaviour of a magnetotactic bacterium. *FEMS Microbiol. Ecol.* 45: 37–45
Taylor, B. L. 1983. Role of proton motive force in sensory transduction by bacteria. *Annu. Rev. Microbiol.* 37: 551–73
Timm, U., Okubo, A. 1991. Gyrotaxis: interaction between alga and microflagellate. To be published
Tsuchiya, Y., Kawakubo, T. 1981. Effect of cell density on thermotaxis of *Paramecium*. *J. Protozool.* 28: 467–69
Wager, H. 1911. On the effect of gravity

upon the movements and aggregation of *Euglena viridis*, Ehrb., and other micro-organisms. *Philos. Trans. R. Soc. London Ser. B* 201: 333–90

Wille, J. J., Ehret, C. F. 1968. Circadian rhythm of pattern formation in populations of a free-swimming organism, *Tetrahymena. J. Protozool.* 15: 789–92

Winet, H., Bernstein, G. S., Head, J. 1984. Observation on the response of human spermatozoa to gravity, boundaries and fluid shear. *Reprod. Fert.* 70: 511–23

Winet, H., Jahn, T. L. 1972. On the origin of bioconvective fluid instabilities in *Tetrahymena* culture systems. *Biorheology* 9: 87–104